Vol. 687: 173–194, 2022
https://doi.org/10.3354/meps14009

MARINE ECOLOGY PROGRESS SERIES
Mar Ecol Prog Ser

Published April 7

Estimating the cost of growth in southern right whales from drone photogrammetry data and long-term sighting histories

Fredrik Christiansen[1,2,3,*], Lars Bejder[2,3,4], Stephen Burnell[5,7], Rhianne Ward[6], Claire Charlton[6]

[1]Aarhus Institute of Advanced Studies, Høegh-Guldbergs Gade 6B, 8000 Aarhus C, Denmark
[2]Zoophysiology, Department of Biology, Aarhus University, C.F. Møllers Allé 3, 8000 Aarhus C, Denmark
[3]Centre for Sustainable Aquatic Ecosystems, Harry Butler Institute, Murdoch University, Murdoch 6150, Western Australia, Australia
[4]Marine Mammal Research Program, Hawaii Institute of Marine Biology, University of Hawaii at Manoa, Kaneohe, HI 96744, USA
[5]Eubalaena Pty. Ltd, Cottesloe 6011, Western Australia, Australia
[6]Centre for Marine Science and Technology, Curtin University, Bentley 6102, Western Australia, Australia

[7]*Present address:* Flourishing Oceans, Minderoo Foundation, Nedlands 6009, Western Australia, Australia

ABSTRACT: Animal body size and growth patterns play important roles in shaping the life history of species. Baleen whales include the largest animals on the planet, with somatic growth costs expected to be substantial. We used unmanned aerial vehicle photogrammetry and long-term individual sighting histories from photo identification (1991–2019) to estimate the cost of somatic growth for southern right whales (SRWs) *Eubalaena australis*. A Richards length-at-age growth model was developed, based on 161 calves, 20 yearlings, 1 juvenile and 23 adults, ranging in age from newborn to 27 yr. Predicted lengths were 4.7 m at birth, 12.5 m at minimum age of first parturition (6 yr) and an asymptotic length of 14.3 m. A volume-at-age curve was estimated from the body volume versus length relationship, and converted to a mass-at-age curve, using data on body tissue composition of North Pacific right whales *E. japonica* (n = 13). The energetic cost of growth was estimated using published estimates of tissue lipid and protein concentrations. The cost of growth for SRWs (in MJ d^{-1}) was 2112 at birth, 544 at 4 mo, 314 at 1 yr (~weaning age), 108 at 5 yr (minimum age of sexual maturity), 51.5 at 10 yr and 5.2 at 30 yr. The cumulative cost to age 30 was 764.3 GJ, but varied widely (458–995 GJ) depending on the tissue energy content. Our estimates represent a healthy SRW population, and provide a baseline to investigate individual and population level impacts of anthropogenic disturbance (including climate change).

KEY WORDS: *Eubalaena australis* · Baleen whales · Body size · Body length · Body mass · Bioenergetics · Growth models · Morphometrics · Life histories · Unmanned aerial vehicle

1. INTRODUCTION

Animal body size and growth patterns play important roles in shaping the life history traits of a species (Blueweiss et al. 1978, Peters 1983, Schmidt-Nielsen 1984), including birth size (Millar 1977), age at first parturition (Wootton 1987), life span (Promislow 1993) and investment in offspring (Reiss 1991). Modelling of animal growth curves provides valuable insight into the energetic costs of growth of an organism throughout its life (Dmitriew 2011, Douhard et al. 2017). Consequently, comparisons of growth curves between populations, and for the same population over time, can provide insights into the energetic effects of environmental (e.g. resource availability) and anthropogenic factors (e.g. disturbance) on animals (Lepage et al. 1998, Madsen & Shine 2000, Stewart et al. 2021). This is particularly relevant in

*Corresponding author: f.christiansen@bio.au.dk

light of global warming, the effects of which are predicted to lead to changes in body size, reproduction rates and abundance of many species (Isaac 2009, Gardner et al. 2011).

Baleen whales include species that are currently the largest animals on the planet (Lockyer 1976). Their low mass-specific metabolic rates and ability to deposit and store large amounts of body energy reserves enables them to endure prolonged periods of fasting in resource-poor winter breeding grounds, and undertake long-distance migrations to high-productivity summer feeding grounds (Brodie 1975, Lockyer 1981b). Despite their large size, baleen whales have substantially lower weight-specific ages at first reproduction compared to other mammals (Wootton 1987). Further, the close relationship between their reproductive cycle and their annual migratory cycle has resulted in gestation and weaning each being completed within a year of impregnation and birth, respectively (Frazer & Huggett 1973, Lockyer 1984). The rapid growth rate of baleen whales will inherently incur substantial energetic costs for the animals, which can only be sustained in an environment where sufficient resources are available to them.

Growth rates in animal body mass, from which energetic costs of somatic growth can be calculated, are generally obtained from mass-at-age or length-at-age data (von Bertalanffy 1938, Brody 1968, Ricker 1979, Kaufmann 1981). Estimating body mass in free-living large whales is logistically difficult, and hence most of our knowledge comes from catch data from scientific and commercial whaling (Lockyer 1976, 1981a,b). With marine ecosystems changing rapidly due to both natural and anthropogenic factors (e.g. climate change) (Crain et al. 2008, Hoegh-Guldberg & Bruno 2010, Doney et al. 2012, Hawkins et al. 2017), some of these data may no longer be representative of the somatic growth of contemporary populations. This issue was recently highlighted in a study examining trends in body lengths of the endangered North Atlantic right whale (NARW) *Eubalaena glacialis*, which showed that body lengths have been decreasing over the past 4 decades as a result of anthropogenic stressors (Stewart et al. 2021). Further, with many baleen whale populations still recovering from 20th century whaling (Mori & Butterworth 2006, Tulloch et al. 2019), somatic growth is likely to slow down as populations approach the carrying capacity of the environment, and the resources needed to support growth become increasingly limited (Kjellqwist et al. 1995, Harding et al. 2018). In light of this, population growth curves and consequent energetic costs of growth need to be updated, based on non-invasive methods that can be applied to vulnerable populations.

In this study, we used non-invasive unmanned aerial vehicle (UAV) photogrammetry methods and long-term sighting histories to estimate the cost of somatic growth in southern right whales (SRWs) *E. australis*. From UAV-derived volume-at-age data, we developed mass-at-age growth curves, using data on tissue mass composition of North Pacific right whales (NPRWs) *E. japonica*. Data on tissue lipid and protein concentration from other baleen whale species were then used to estimate the cost of growth for SRWs.

2. MATERIALS AND METHODS

A stepwise modelling approach was developed to estimate the cost of somatic growth in SRWs (Fig. 1).

2.1. Data collection

Body morphometric measurements of SRWs were obtained using UAV photogrammetry methods at the Head of Bight (HoB) breeding/calving ground in South Australia between late June and late September 2016–2019. A DJI Inspire 1 Pro multirotor UAV (diameter without propellers: 56 cm, weight: 3.4 kg, www.dji.com) with a 16 Megapixel Zenmuse X5 micro four-thirds camera with an Olympus M.Zuiko 25 mm f1.8 lens was flown above SRWs at altitudes of 16.5–64.0 m (mean ± SD = 34.7 ± 4.71 m, n = 5190) to photograph the dorsal side of the whales as they surfaced to breathe. The altitude of the UAV above sea level was recorded with a LightWare SF11/C laser range finder (Lightware Optoelectronics, weight: 35 g) attached to the UAV. The UAV was only flown during favourable weather conditions (no rain and wind speeds <15 knots). Following the protocol of Christiansen et al. (2018), all photographs were graded based on multiple criteria: camera focus, degree of body roll, degree of body arch, body pitch, body length measurability (accuracy of body length measurement) and body width measurability (accuracy of body width measurements). Photograph image grading was done on a scale from 1 to 3, where 1 was good quality, 2 was medium quality, and 3 was poor quality. Only images that received a quality grade of 1 or 2 for body length measurability (mean error <0.38%) and body width measurability (mean error <2.31%), and less than 2 grades of score 2 for pitch, arch and roll combined were used in the analyses (Christiansen et al. 2018).

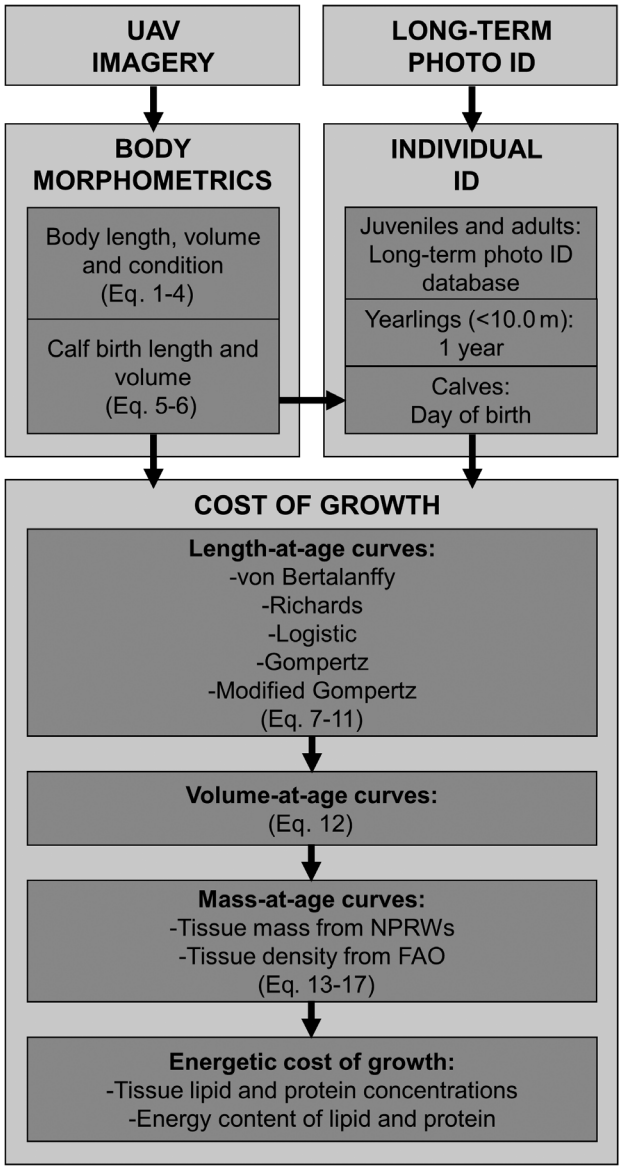

Fig. 1. Structure of the modelling framework used to estimate the cost of somatic growth for southern right whales. Each section is described in the main text under similar subheaders. UAV: unmanned aerial vehicle; NPRWs: North Pacific right whales; FAO: Food and Agriculture Organization of the United Nations (data from Charrondiere et al. 2012)

Individual whales were identified from the aerial photographs using the unique callosity patterns on their heads (Payne et al. 1983) and were classified as calves, yearlings, juveniles, adults, late-pregnant (about to give birth within the same breeding season) or lactating females. Calves and lactating females were classified based on their relative size (calves are <2/3 the length of their mothers; Christiansen et al. 2018) and close association with each other. All calves measured in this study were born during the breeding season of the sampling year and were hence <120 d old. Yearlings, juveniles and adults (presumed sexually mature animals that were not late-pregnant or lactating) were separated based on the following body length thresholds: yearlings, <10.0 m; juveniles, ≥10.0 and <12.0 m; adults, ≥12.0 m (Christiansen et al. 2020a). Unaccompanied adults that were later observed with a dependent calf within the same breeding season were classified as late-pregnant. It is important to note that there is individual variation around the length and age at which individual baleen whales become sexually mature (Chittleborough 1955), which means that some larger juveniles might have been classified as adults, and some smaller adults might have been classified as juveniles.

2.2. Body morphometrics and allometric growth patterns

From the selected aerial photographs, the body length and widths (at 5% increments along the body of the whale) were measured, in pixels, using the approach of Christiansen et al. (2016). Measurements were taken using a custom-written script in R v.4.0.3 (R Core Team 2020; free script available from Christiansen et al. 2016). Measurements were converted from pixels to metres using the known resolution of the pictures (4608 × 3456 pixels), the size of the camera sensor (17.3 × 13 mm), the altitude of the UAV (obtained from the range finder) and the focal length of the camera (25 mm) (for details, see Christiansen et al. 2018).

The effect of body length on several body morphometrics was investigated using generalized additive models (GAMs) with a thin plate regression spline smoother in R. A separate model was fitted to each of the following allometric relationships: (1) head width (distance between eyes) against body length, (2) head length (rostrum to midpoint between eyes) against body length, (3) blowhole distance (rostrum to blowhole) against body length and (4) fluke width against body length. A density histogram was then produced from the metric that showed that strongest allometric relationship, with calves, juveniles (including yearlings) and adults (including pregnant and lactating females) plotted separately to determine the threshold length values (intersections between density distributions) to differentiate between the different maturity classes. While these threshold values were not used to classify whales in the present study, they could potentially be used in studies

where absolute body length measurements are not available.

2.3. Body volume and condition

For each body width (W) measurement, the corresponding height (H, dorso-ventral distance) was calculated using the known height:width ratio of SRWs (Christiansen et al. 2019). The body volume ($BV_{\mathrm{Total},i}$) of each whale i was then estimated from the sum of the volume of each body segment ($BV_{s,i}$) by modelling each segment s (the body section between 2 adjacent width measurements) as a series of infinitesimal ellipses (Christiansen et al. 2019):

$$BV_{Total,i} = \sum_{s=1}^{20} BV_{s,i} \tag{1}$$

where BV_s is given by:

$$BV_{s,i} = BL_i \times 0.05 \times \int_0^1 \pi \times \frac{W_{\mathrm{A},s,i} + (W_{\mathrm{P},s,i} - W_{\mathrm{A},s,i}) \times x}{2} \times \frac{H_{\mathrm{A},s,i} + (H_{\mathrm{P},s,i} - H_{\mathrm{A},s,i}) \times x}{2} dx \tag{2}$$

where $W_{\mathrm{A},s,i}$ and $H_{\mathrm{A},s,i}$ are the anterior width and height measurements of body segment s for individual i, and $W_{\mathrm{P},s,i}$ and $H_{\mathrm{P},s,i}$ are the posterior width and height measurements of segment s for individual i, respectively. To account for the gradual decrease in height and width towards the end points of the animal, the segments closest to the rostrum (0–5% body length [BL] from the rostrum [hereafter just '%BL']) and the end of the tail region (85–100%BL) were modelled as elliptical cones (Christiansen et al. 2019).

The relative body condition (BC_i) was calculated for each whale i using the formula of Christiansen et al. (2018):

$$BC_i = \frac{BV_{\mathrm{Obs},i} - BV_{\mathrm{Exp},i}}{BV_{\mathrm{Exp},i}} \tag{3}$$

where $BV_{\mathrm{Obs},i}$ is the observed (measured) body volume of whale i, in m^3, and $BV_{\mathrm{Exp},i}$ is the expected body volume of whale i, in m^3, given by the log–log relationship between body volume and body length:

$$\log(BV_{\mathrm{Exp},i}) = \alpha + \beta \times \log(BL_i) \tag{4}$$

where α and β represent the intercept and slope parameters, respectively, of the linear model. Our body condition metric represents the difference in relative body volume (expressed as a proportion) of an individual whale compared to the expected body volume of an average whale of the same body length (the mean body volume predicted from Eq. 4) from the sample population (based on all the measured SRWs in this study). For example, a whale with a body condition of 0.20 (or 20%) has a body volume that is 20% higher than the average (expected) body volume of a whale of the same body length, while a whale with a body condition of −0.20 (or −20%) has a body volume that is 20% lower than the average (expected) body volume of a whale of the same body length. The body volume of a whale with body condition 0 (or 0%) is the same as the average (expected) body volume of the sample population, while accounting for its body length (structural size).

2.4. Age estimation

The age of young calves (<4 mo) was estimated from repeated measurements of body volume from individual animals (identified using the callosity pattern of their mothers, Payne et al. 1983) throughout the winter breeding season. First, calf volume at birth (CBV) was predicted from calf birth length (CBL) by modifying Eq. (4):

$$\mathrm{CBV}_i = \exp[\alpha + \beta \times \log(CBL_i)] \tag{5}$$

where CBL was predicted from maternal length (ML) using the linear relationship ($F_{2,54} = 75.9$, $p < 0.001$, $R^2 = 0.738$) estimated by Christiansen et al. (2022):

$$CBL_i = 0.891 + 0.283 \times ML_i \tag{6}$$

The day of birth (as day of year) of calves was then calculated following the approach of Christiansen et al. (2018), by fitting linear models to the relationship between calf volume and day of year, 1 for each individual calf, and then replacing calf volume in the resulting models with CBV from Eq. (5). Only calves with a minimum of 4 measurements and at least 20 d between the first and last measurement were used for analysis (Christiansen et al. 2018).

Individuals identified as yearlings (non-calves with body lengths <10.0 m) were all given an age of 1 yr (the assumed minimum age), although the exact birth date was unknown. The ages of juveniles and adults (including pregnant and lactating females) were determined by matching the aerial photographs of their unique callosity patterns (Payne et al. 1983) with the HoB long-term identification database

(1975–2019) held by the Great Australian Bight Right Whale Study (GABRWS, www.gabrightwhales.com). Measured whales without age data were excluded from the following analyses.

2.5. Length-at-age and volume-at-age curves

To predict the body length BL_t (m) of SRWs at age t (yr), 5 different growth functions (models) were fitted to the length-at-age data:

von Bertalanffy (von Bertalanffy 1938):

$$BL_t = L_\infty(1-e^{-k(t-t_0)}) \quad (7)$$

Richards (Pauly 1979):

$$BL_t = L_\infty(1-e^{-k(t-t_0)})^p \quad (8)$$

Logistic (Ricker 1979):

$$BL_t = \frac{L_\infty}{1+e^{-k(t-t_0)}} \quad (9)$$

Gompertz (Gompertz 1825):

$$BL_t = L_\infty e^{-e^{k(t-t_0)}} \quad (10)$$

Modified Gompertz (Laird 1966):

$$BL_t = L_0 e^{k/b(b(1-e^{-bt}))} \quad (11)$$

where L_∞ is the asymptotic body length, k is a growth velocity constant, t_0 is a time constant, p is a shape constant, L_0 is the body length at birth, and b is the rate of exponential decay of the growth rate. Different transformations of the age variable were investigated, including log, square-root and cube-root. Parameter values for all models were estimated using least squares regression ('minpack.lm' package v.1.2-1 in R, Elzhov et al. 2016), and 95% confidence intervals were obtained using bootstrap resampling ('nlstools' package v.2.0-0 in R, Baty et al. 2015) with 1000 iterations. Although baleen whales exhibit sexual dimorphism, with females reaching asymptotic lengths that are generally 5% longer than males (Mesnick & Ralls 2018), small sample size prevented separate growth models to be fitted to each sex.

To avoid pseudo-replication, only a single body length measurement from each non-calf individual was included in the analyses. However, since calves were expected to grow significantly throughout the study period (within a breeding season, Christiansen et al. 2018), repeated measurements of body length from the same calves were included in the analyses. To assess whether this approach introduced a bias in our model parameter estimates, we ran a bootstrapping simulation where only a single body length measurement for each calf was randomly included in each iteration. By doing this 1000 times, and extracting the parameter values for each iteration, we could obtain a density distribution around each model parameter value, from which we could test the robustness of the model to repeated measurements. The same approach was used to quantify the effect of measurement errors in the UAV-derived body length estimates. Christiansen et al. (2018) estimated the mean ± SD measurement errors inherent from the altimeter of our UAV system to be 0.73 ± 0.49 cm. The coefficient of variation in body length measurements associated with the different length measurability scores (the ability to accurately pinpoint the tip of the rostrum and the notch of the tail fluke of whales) were 0.30 and 0.38% for quality 1 and 2, respectively (Christiansen et al. 2018). Finally, the mean measurement error between photographs of the same whale within the same day was 4.75 ± 3.67% (Christiansen et al. 2018). By randomly allocating new body length values to the measured whales (1000 times), based on these error distributions, and refitting the best-fitting growth model, we could obtain a distribution of parameter values for the best-fitting model and compare it to the original model.

Model selection was based on visual interpretation of the growth curves in relation to the measured length-at-age data, where the aim was to find a model that both fitted the observed data for each age class (calves, yearlings, juveniles and adults), and produced biologically realistic predictions of *CBL*, length at minimum age of sexual maturity, length at minimum age of first parturition and asymptotic body length. The predicted *CBL* values (age = 0) were evaluated against the possible range of birth sizes for SRWs from Eq. (6) (Christiansen et al. 2022). Length at minimum age of first parturition was based on Christiansen et al. (2020a), who estimated the length threshold for sexual maturity of SRWs to be ~12.0 m, based on measurements from pregnant and lactating females. Charlton (2017) estimated the corresponding minimum age at first parturition for the South Australia population to be 6 yr (females becoming sexually mature at 5 yr). In regards to asymptotic length, the duration of the GABRWS long-term ID database (1975–2019) set an upper age limit of the length-at-age data of 28 yr. With the longevity of

SRWs likely to be much higher (here assumed to be ~80 yr, based on the longest recorded age of a right whale, which was 65 yr, and the recorded maximum ages of other baleen whales; see Hamilton et al. 1998 for review), it is unlikely that our length-at-age data will capture the upper limit in body length of SRWs. To overcome this limitation, we extrapolated our length-at-age curves up to 80 yr of age, and compared the resulting (predicted) model length range with the observed distribution of body lengths measured for adult SRWs (including pregnant and lactating females) in our photogrammetry data set.

The best-fitting length-at-age curve was used to create a volume-at-age curve, using the estimated log–log relationship between body volume and body length (Eq. 4):

$$BV_t = \exp[\alpha + \beta \times \log(BL_t)] \quad (12)$$

From the best-fitting length-at-age and volume-at-age curves, the growth rates in length and volume of SRWs were estimated throughout their lifetime (i.e. 80 yr). The resulting volume-at-age curve is representative of SRWs in average body condition ($BC = 0$) based on 4 seasons of sampling at the HoB breeding/calving ground. Since our sampling period (late June to late September) represents the primary breeding/calving season for SRWs in Australian waters, with individuals arriving in good body condition and leaving in poor body condition (Christiansen et al. 2018, 2020a), this should provide a good baseline for SRWs in Australian waters, and a comparison for global populations.

2.6. Mass-at-age curves

To obtain mass-at-age curves for SRWs, the volume-at-age curve was multiplied by the average tissue density of SRWs in average body condition ($BC = 0$). The average tissue density was estimated using published data from Omura et al. (1969), who obtained detailed measurements of body morphometrics, mass and tissue composition (relative mass of blubber, muscle, viscera and bones) for 13 NPRWs caught during their summer feeding season in scientific whaling operations between 1961 and 1968, a population which is now endangered (Cooke & Clapham 2018). Morphometric measurements included body mass of each body tissue component (to the nearest kilogram, not including the weight of blood and other body fluids lost during the processing of the carcass), total body length (to the nearest decimetre) and half girths (to the nearest centimetre) measured at 3 locations: the anterior insertion of the pectoral fins ($G_{25\%BL}$, at ~25 %BL from the rostrum), across the umbilicus ($G_{50\%BL}$, at ~50 %BL from the rostrum) and across the anus ($G_{72\%BL}$, at ~72 %BL from the rostrum) (Omura et al. 1969). The BV of the dead whales was calculated from the BL and 3 girth measurements (G), using the formula of Christiansen et al. (2019) ($F_{4,81} = 70050$, $p < 0.001$, $R^2 = 0.999$):

$$\log(BV_i) = -2.764 + 1.003 \times \log(BL_i) + 0.809 \times \log(G_{25\%BLi}) + 0.814 \times \log(G_{50\%BLi}) + 0.294 \times \log(G_{72\%BLi}) \quad (13)$$

The body condition of the dead whales was calculated (Eq. 3) using the estimated body volume from their length and girths (Eq. 13) and the expected body volume of an average SRW based on their body length (Eq. 4).

The body tissue composition of baleen whales varies with both the size (i.e. body length) and body condition of animals (Lockyer 1981b, Vikingsson 1995). With right whales having a significantly higher proportion of blubber compared to other baleen whale species (Lockyer 1976), we assumed that variation in body condition was directly related to changes in the relative blubber mass of individuals. Consequently, we assumed that muscle, visceral and bone tissue mass were determined only by the structural body size (body length) of individuals. Based on these assumptions, we modelled the tissue mass ($M_{\text{Tissue},i}$) of muscle, viscera and bones for a whale (i) of a given body length (BL_i) as:

$$M_{\text{Tissue},i} = \exp[\alpha + \beta \times \log(BL_i)] \times P_{\text{Tissue}} \times 10^3 \quad (14)$$

where the expression $\exp[\alpha + \beta \times \log(BL_i)]$ is equivalent to the expected body volume ($BV_{\text{exp},i}$) of an individual (i) in average body condition ($BC = 0$, given by Eq. 4), and P_{Tissue} is the proportion of the volume of the whale that is comprised of a given tissue. P_{Tissue} was estimated for muscle, viscera and bones by artificially varying its relative contribution to total volume from 0 to 100 %, in increments of 0.1 %, and then comparing the resulting tissue mass of each whale with its actual measured tissue mass in the NPRW data set (Omura et al. 1969). The sum of the residuals ($M_{\text{Tissue},Obs,i} - M_{\text{Tissue},Exp,i}$) of all individuals was calculated for each tissue proportion, and the proportion that resulted in the lowest error (smallest residual sum) was selected. To test our assumption that tissue mass for muscle, viscera and bones was only affected

by structural size (body length) and not body condition, the resulting tissue mass residuals were modelled against the calculated body condition of the individual, using linear models.

The blubber mass ($M_{\mathrm{Blubber},i}$), in kg, of an SRW (i) of a given body length (BL_i) and body condition (BC_i) was then estimated from:

$$M_{\mathrm{Blubber},i} = [(1+BC_i)\times \exp(\alpha+\beta\times\log(BL_i)) - \frac{M_{\mathrm{Muscle},i}}{D_{\mathrm{Muscle}}} - \frac{M_{\mathrm{Viscera},i}}{D_{\mathrm{Viscera}}} - \frac{M_{\mathrm{Bones},i}}{D_{\mathrm{Bones}}}]\times D_{\mathrm{Blubber}}\times 10^3 \quad (15)$$

where $M_{\mathrm{Muscle},i}$, $M_{\mathrm{Viscera},i}$, and $M_{\mathrm{Bones},i}$ is the predicted mass of muscle, viscera and bones of whale i (given by Eq. 14) and D_{Blubber}, D_{Muscle}, D_{Viscera}, and D_{Bones} are the tissue densities of blubber, muscle, viscera and bone tissue. We used the published tissue densities (kg m^{-3}) from FAO (blubber = 700, muscle = 960, bones = 720, viscera = 930, Charrondiere et al. 2012). The average tissue density ($D_{\mathrm{Total},i}$), in kg m^{-3}, of a whale (i) could then be calculated from:

$$D_{\mathrm{Total},i} = (M_{\mathrm{Blubber},i} + M_{\mathrm{Muscle},i} + M_{\mathrm{Viscera},i} + M_{\mathrm{Bones},i})/BV_i \quad (16)$$

Finally, a mass-at-age curve was developed for SRWs from the predicted body volume (BV_t) resulting from the volume-at-age curves (Eq. 12) and the average tissue density (D_{Total}, Eq. 16) for an animal of average body condition ($BC = 0$):

$$M_t = BV_t \times D_{\mathrm{Total},t} \quad (17)$$

It is worth noting that our model is based on catch records of NPRWs where blood and fluid loss was not accounted for (Omura et al. 1969), which in baleen whales generally constitute ~6% of the total body mass (Lockyer 1976). From the estimated mass-at-age curve (Eq. 17), the daily growth in body mass of SRW could be estimated. From the known relationship between tissue mass and body length (Eqs. 14 & 15), the daily growth in mass of each tissue type could be estimated.

2.7. Energetic cost of growth

From the estimated mass and daily growth rates of the different body tissues, we calculated the energy content of each tissue and the consequent energy requirement for somatic growth. The energy content of the different tissues (blubber, muscle, viscera and bones) was estimated from the assumed lipid and protein concentration of the specific tissues (similar to Lockyer et al. 1985 and Vikingsson 1990). Unfortunately, few data exist on the tissue energy content of right whales, so instead we used published values from fin *Balaenoptera physalus*, sei *B. borealis* and minke whales *B. acutorostrata* (Lockyer et al. 1985, Lockyer 1987, Vikingsson 1990, Vikingsson et al. 2013a). Since lipid and protein concentrations in blubber, muscle and visceral tissues are known to vary across the body of whales, both seasonally and also between species and reproductive classes (Lockyer et al. 1984, 1985, Lockyer 1987, Aguilar & Borrell 1990, Vikingsson 1990, Vikingsson et al. 2013a), a range of values was modelled for each tissue type (Table 1), and the resulting cumulative energetic cost of growth from birth to 30 yr of age was calculated (see Fig. S1 in the Supplement at www.int-res.com/articles/suppl/m687p173_supp.pdf). To account for the negative correlation between protein and lipid concentrations in blubber, muscle and viscera tissue (see Fig. S2), the lipid concentrations were artificially varied within their published range of values (Table 1), and the corresponding protein concentration was predicted from the linear relationship between the 2 variables (see Fig. S2). Only 1 published value on protein concentration in bone was found for fin whales (Lockyer 1987), and hence this value was fixed in the model simulations (Table 1). That a single value for bone protein concentration was used in our analyses should not be misinterpreted as statistical confidence, as this is purely the result of insufficient data. The calorific equivalents of lipids and protein were assumed to be 39 539 kJ kg^{-1} (9450 kcal kg^{-1}) and 23 640 kJ kg^{-1} (5650 kcal kg^{-1}) wet weight, respectively (Brody 1968, Lockyer et al. 1985).

3. RESULTS

3.1. Sample size and effort

SRW body morphometric data were collected at HoB on 173 d between 2016 and 2019 between June and September (Table 2). A total of 9019 measurements of whales was obtained. However, after quality filtering (based on camera focus, body posture and body contour clarity) 5372 measurements (~60%) of whales remained from 791 individuals (Table 2). The great majority (94.6%) of measurements was of mothers and calves. The body length of the measured SRWs ranged between 3.9 and 8.8 m (mean ± SD = 6.3 ± 0.8, n = 2567) for calves, between

Table 1. Modelled values of lipid and protein concentrations in blubber, muscle, viscera and bone tissue of southern right whales, based on published values from fin, sei and minke whales. For the bootstrapping simulations (Fig. S1), lipid values were incrementally increased from the minimum to the maximum within each range, and the corresponding protein concentrations were predicted from the linear relationships between the 2 variables for each tissue type (Fig. S2). The calorific equivalents of lipids and protein were assumed to be 39 539 kJ kg^{-1} (9450 kcal kg^{-1}) and 23 640 kJ kg^{-1} (5650 kcal kg^{-1}) wet weight, respectively (Brody 1968, Lockyer et al. 1985). Sources: Lockyer et al. (1985), Lockyer (1987), Vikingsson (1990), Vikingsson et al. (2013a)

Tissue	Lipid concentration (% wet mass)		Protein concentration (% wet mass)		Energetic cost for growth (kJ kg^{-1})
	Mean ± SD	Range	Mean ± SD	Range	Mean
Blubber	62.6 ± 14.8	19.2–81.3	10.2 ± 3.9	3.5–20.4	27163
Muscle	11.4 ± 8.0	1.9–33.1	22.1 ± 2.3	18.1–26.1	9732
Viscera	75.8 ± 9.6	59.6–92.8	3.7 ± 1.7	1.2–8.2	30845
Bones	21.8 ± 3.8	18.4–25.9	24.8[a]	24.8[a]	14482

[a]Only 1 published value of bone protein concentration was found, and hence this value was fixed

Table 2. Sample composition of the southern right whales measured at the Head of Bight, South Australia, by unmanned aerial vehicle photogrammetry by year and reproductive class. The sampling effort in each year is also provided. n = 5372 whales measured (791 individuals, including 26 females that were measured both as pregnant and lactating)

Year	Dates		Sampling effort		Number of whales measured (individuals)					
	Start	End	Period	Days	Calves	Yearlings	Juveniles	Adults	Pregnant	Lactating
2016	24 Jun	25 Sep	93	49	1090 (89)	1 (1)	17 (13)	39 (20)	3 (3)	865 (84)
2017	13 Jul	25 Sep	74	38	405 (87)	0 (0)	6 (5)	22 (17)	1 (1)	410 (85)
2018	23 Jun	24 Sep	93	41	410 (88)	31 (10)	13 (10)	53 (30)	31 (11)	537 (90)
2019	28 Jun	24 Sep	88	45	662 (67)	10 (5)	18 (9)	24 (14)	19 (11)	705 (67)
Total	24 Jun	25 Sep	93	173	2567 (331)	42 (16)	54 (37)	138 (81)	54 (26)	2517 (326)

8.9 and 9.9 m (9.4 ± 0.3 m, n = 42) for yearlings, between 10.1 and 12.0 m (10.9 ± 0.6 m, n = 54) for juveniles, between 12.0 and 14.6 m (13.3 ± 0.8, n = 138) for adults, between 12.6 and 14.8 m (13.7 ± 0.6, n = 54) for late-pregnant females, and between 11.7 and 16.2 m (14.0 ± 0.6 m, n = 2517) for lactating females (Fig. S3).

3.2. Body morphometrics and allometric growth patterns

There was a significant non-linear relationship between SRW head width and body length ($F_{4.87,4.99}$ = 1889, p < 0.001, R^2 = 0.638, Fig. 2A), head length and body length ($F_{6.58,6.94}$ = 5202, p < 0.001, R^2 = 0.871, Fig. 2B), rostrum to blowhole distance and body length ($F_{6.64,6.95}$ = 1565, p < 0.001, R^2 = 0.670, Fig. 2C) and fluke width and body length ($F_{4.70,4.95}$ = 370, p < 0.001, R^2 = 0.256, Fig. 2D). The relative head width of SRWs increased linearly with body length from ~17 %BL for small calves to ~21 %BL for large juveniles, but started to decrease again as the animals reached the minimum length at sexual maturity at ~12 m body length down to about 20 %BL for large (16 m long) adults (Fig. 2A). The relative head length and blowhole distance for calves was centred at ~19 and ~14 %BL, respectively, but increased linearly for juveniles until it plateaued for mature animals at ~24 and ~18 %BL, respectively (Fig. 2B,C). The relative fluke width of SRWs increased curvilinearly for calves from ~27 to ~38 %BL, but then decreased linearly for juveniles and adults down to ~34 %BL for large adults (Fig. 2D).

Among the 4 morphometric variables investigated (head width, head length, blowhole distance and fluke width), relative head length showed the strongest allometric relationship. There was a significant non-linear relationship between SRW body length and relative head length ($F_{5.00,5.00}$ = 11488, p < 0.001, R^2 = 0.915, Fig. 3A). Plotting the density distribution of relative head length for calves, immature (yearlings and juveniles) and mature (adults, pregnant and lactating) whales, threshold (cut-off) values (intersections between the different distributions) were identified at 20.36 and 22.88 %BL head lengths to distinguish calves from juveniles, and to distinguish juveniles from adults, respectively (Fig. 3B).

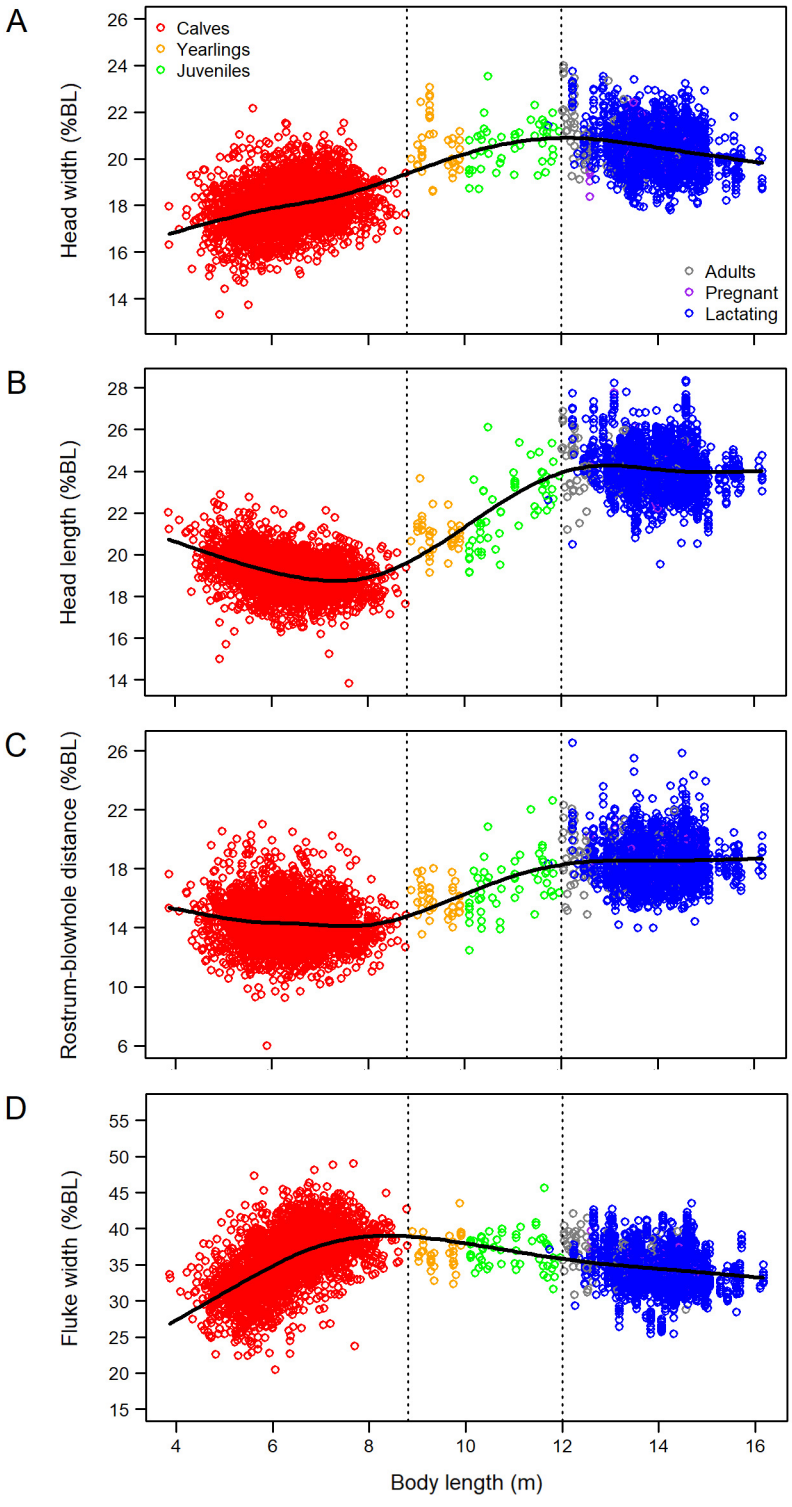

Fig. 2. Allometric relationship between southern right whale body length and relative (A) head width (eye–eye distance), (B) head length (rostrum–eyes distance), (C) rostrum–blowhole distance and (D) fluke width. Colours indicate the reproductive classes (see keys). The solid lines represent the fitted value of the generalized additive models. The dotted vertical lines indicate the length threshold values for yearling/juveniles (8.8 m) and mature animals (12.0 m). n = 5346 measurements

3.3. Body volume and condition

The estimated body volume of SRWs varied between 0.89 and 11.88 m^3 (mean ± SD = 4.60 ± 1.89 m^3) for calves, between 11.57 and 21.34 m^3 (16.3 ± 2.86 m^3) for yearlings, between 14.71 and 38.8 m^3 (22.39 ± 4.38 m^3) for juveniles, between 25.65 and 64.85 m^3 (41.00 ± 8.88 m^3) for adults, between 29.85 and 65.85 m^3 (49.84 ± 8.34 m^3) for pregnant females and between 24.75 and 77.48 m^3 (47.17 ± 7.89 m^3) for lactating females (Fig. 4A). There was a significant ($F_{1,5370}$ = 801 472, $p < 0.001$, R^2 = 0.993) positive relationship between body volume (BV) and body length (BL) on the log-log scale:

$$\log(BV_{\mathrm{Exp},i}) = -4.115 + 3.016 \times \log(BL_i) \quad (18)$$

The body condition of the measured whales ranged from −28.8 to 58.0%, with a mean of 0.0 ± 10.1%.

3.4. Age estimation

Age was estimated for 161 calves that fulfilled the criteria for minimum sample size (≥4 measurements) and sample duration (≥20 d between first and last sample). Calves ranged in body length from 4.25 to 8.77 m, and were estimated to be between 0 and 112 d old (Fig. 5). The volume growth rates of calves varied from 0.026 to 0.122 $m^3\ d^{-1}$, with a mean ± SD of 0.075 ± 0.016 $m^3\ d^{-1}$ (Fig. S4A), while the length growth rates varied from 0.017 to 0.056 m d^{-1}, with a mean of 0.033 ± 0.006 m d^{-1} (Fig. S4B). A total of 80 yearlings (20 individuals) were measured. Yearlings varied in body length from 8.31 to 10.07 m (Fig. 5). One juvenile of known age was measured, and was 11.14 m long and 4 yr old (Fig. 5). A total of 23 adults (including late-pregnant and lactating females) of known age were measured. The adults ranged in body length from 12.09 to 15.44 m, and were between 8 and 27 yr in age (Fig. 5).

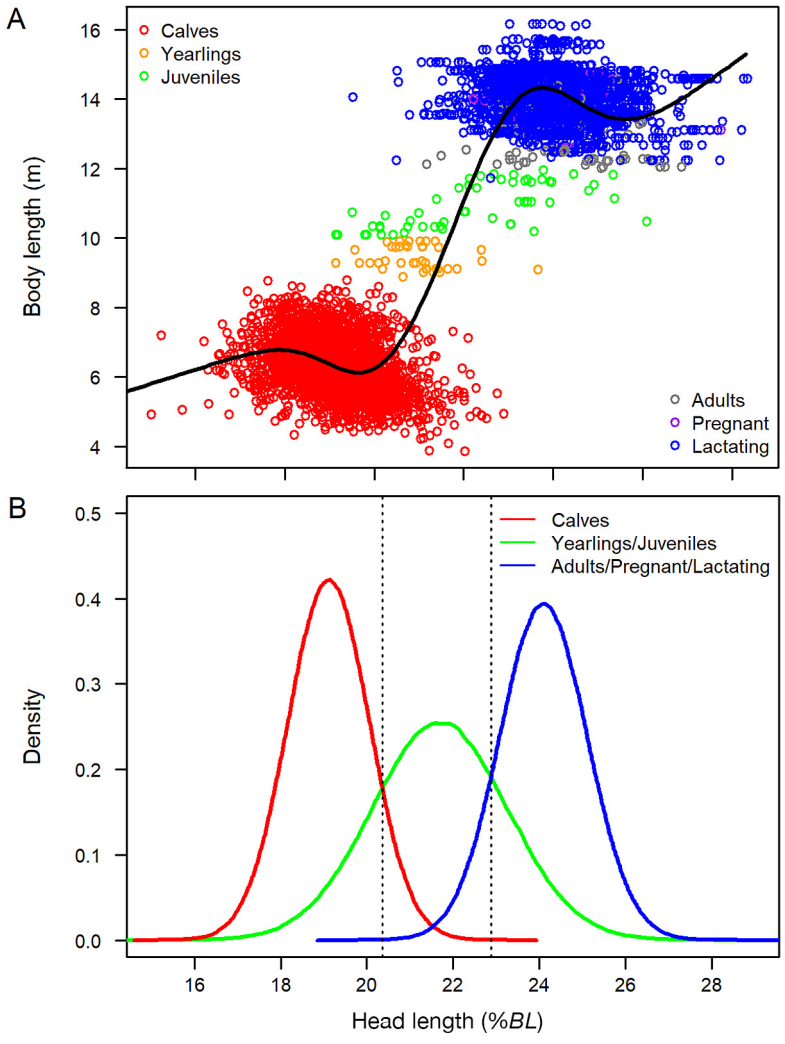

Fig. 3. (A) Body length as a function of relative head length for southern right whales. Colours indicate the reproductive classes (see key). The solid lines represent the fitted value of the generalized additive model. n = 5346 measurements. (B) Density distributions of relative head length for southern right whales. Colours indicate the maturity classes. The dotted vertical lines indicate the head length threshold values to distinguish between calves and immature animals (20.36 %BL, where BL is body length) and between immature and mature animals (22.88 %BL)

minimum age of first parturition and asymptotic length (Table 3, Figs. S5–S9). Based on simplicity and model fit, the non-transformed Richards growth curve was selected (Fig. 5). The bootstrapping simulation, which removed repeated measurement from the same individuals, resulted in slightly different estimates for L_∞ (14.286 compared to 14.138), k (0.106 compared to 0.129), t_0 (−0.018 compared to −0.021) and p (0.179 compared to 0.186) (Fig. S10). The model parameters were robust to measurement errors in body length (Fig. S11). Using the mean parameter estimates from the bootstrapping simulation, the length-at-age growth model for SRWs in South Australia was (Fig. 5A,C,E, Table 4):

$$BL_t = 14.286\{1-e^{-0.106[t-(-0.018)]}\}^{0.179}$$

Upper 95 % CI:

$$BL_t = 14.527\{1-e^{-0.128[t-(-0.022)]}\}^{0.173} \quad (19)$$

Lower 95 % CI:

$$BL_t = 14.057\{1-e^{-0.085[t-(-0.015)]}\}^{0.185}$$

which combined with Eq. (18) gave the corresponding volume-at-age curve (Fig. 5B,D,F, Table 4):

$$BV_t = \exp\{-4.115 + 3.016 \times \log[14.286(1-e^{-0.106(t-(-0.018))})^{0.179}]\}$$

Upper 95 % CI:

$$BV_t = \exp\{-4.115 + 3.016 \times \log[14.527(1-e^{-0.128(t-(-0.022))})^{0.173}]\} \quad (20)$$

Lower 95 % CI:

$$BV_t = \exp\{-4.115 + 3.016 \times \log[14.057(1-e^{-0.085(t-(-0.015))})^{0.1085}]\}$$

3.5. Length-at-age and volume-at-age curves

Several of the growth models fitted the length-at-age data well (Table 3, Figs. S5–S9). For all models, the log-transformation performed poorly, by either not converging or by predicting birth lengths of zero (Table 3). With the exception of the Richards growth model (Fig. S6), the non-transformed models predicted unrealistically low asymptotic lengths (Table 3). The remaining models all produced biologically reasonable estimates of *CBL*, length at minimum age of sexual maturity, length at

Based on the above models, the mean predicted length at birth for SRWs in South Australia was 4.7 m (95 %CI = 4.1–5.3 m), the mean length at minimum age of sexual maturity (age = 5) was 12.2 m (11.6–12.8 m), mean length at minimum age of first parturition (age = 6) was 12.5 m (11.9–13.1 m), and mean asymptotic length was 14.3 m (14.1–14.5 m) (Table 4, Table S1). The growth rate in body length and volume of SRWs decreased exponentially with age (Fig. 5, Table 4). The rate of growth in body length decreased from 11.87 cm d^{-1} at birth, to 3.04 cm d^{-1} at 1 mo of age, to 1.09 cm d^{-1} at 4 mo (when most calves will

have started their migration back to the feeding grounds), to 0.43 cm d^{-1} at 1 yr (age of weaning), to 0.09 cm d^{-1} at the minimum age of sexual maturity (5 yr) (Fig. 5A,C, Table 4).

Assuming a fixed body condition (BC = 0), the volume growth rate of SRWs in South Australia decreased from 0.134 m^3 d^{-1} at birth, to 0.062 m^3 d^{-1} at 1 mo of age, 0.035 m^3 d^{-1} at 4 mo, 0.020 m^3 d^{-1} at 1 yr and 0.007 m^3 d^{-1} at minimum age of sexual maturity (Fig. 5B,D, Table 4; Table S1). Mature whales (>6 yr) had a low growth rate in both length and volume, at 0.04 cm d^{-1} and 0.003 m^3 d^{-1} at 10 yr old, respectively, and at 0.003 cm d^{-1} and 0.0003 m^3 d^{-1}, at 30 yr, respectively (Fig. 5E,F, Table 4; Table S1).

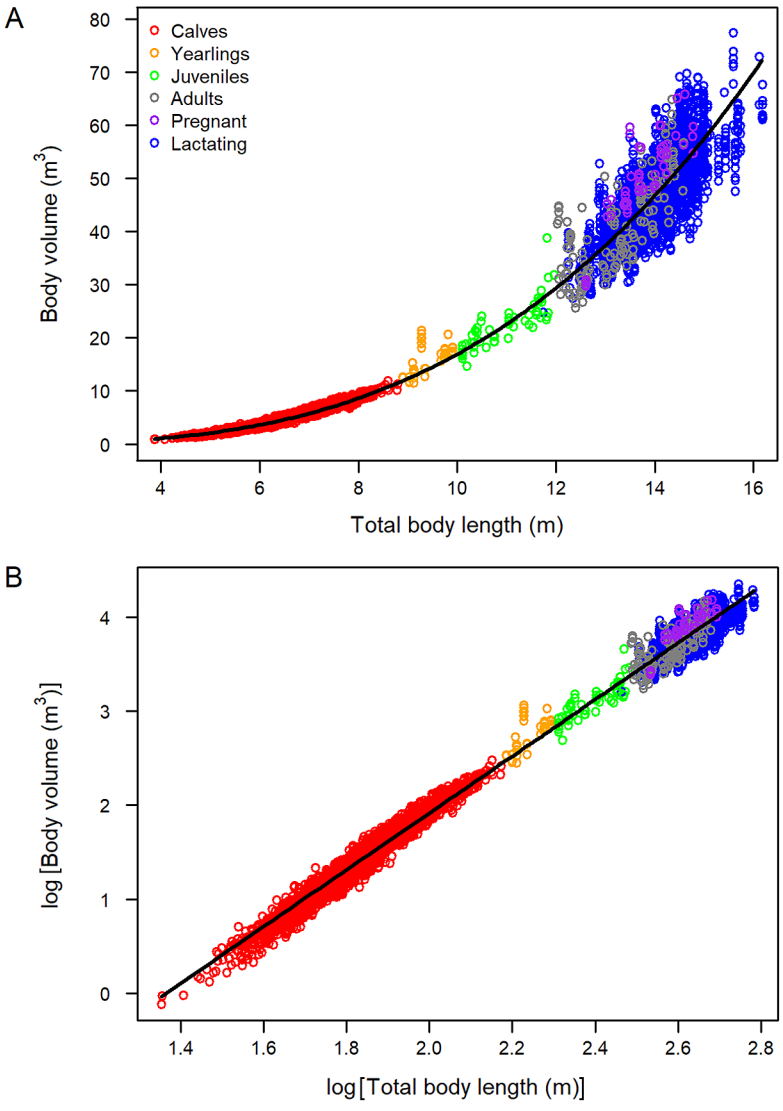

Fig. 4. (A) Southern right whale body volume as a function of body length. The solid black line represents the back-transformed fitted values of the linear model. (B) Log–log relationship between body volume and body length for the same data set, with the solid black line representing the fitted values of the linear model. Colours indicate the reproductive classes (see key); n = 5372 body volume and length measurements (see Table 1 for sample composition)

3.6. Mass-at-age curves

The calculated body condition of the NPRWs ranged from −1.4 to 51.4%, while the UAV-derived body condition estimates of the SRWs ranged from −28.8 to 58.0%. There was hence considerable overlap in the body condition ranges of the 2 sample populations, which justifies the extrapolation of the tissue mass relationships from NPRWs to SRWs. The volume proportions that best fitted the measured tissue weights of NPRWs (Omura et al. 1969) were 36.3% blubber, 28.2% muscle, 10.2% viscera and 12.5% bone (Fig. 6A). Comparing the tissue mass residuals against body condition, there was no effect on muscle, bone and viscera tissue (Fig. 6B). Hence, muscle ($M_{\mathrm{Muscle},i}$), viscera ($M_{\mathrm{Viscera},i}$) and bone mass ($M_{\mathrm{Bones},i}$), in kg, could be predicted directly from the body length (BL_i), or structural size, of the animals (Fig. 7A):

$$M_{\mathrm{Muscle},i} = \exp[-4.115 + 3.016 \times \log(BL_i)] + 0.282 \times 10^3 \quad (21)$$

$$M_{\mathrm{Viscera},i} = \exp[-4.115 + 3.016 \times \log(BL_i)] + 0.102 \times 10^3 \quad (22)$$

$$M_{\mathrm{Bones},i} = \exp[-4.115 + 3.016 \times \log(BL_i)] + 0.125 \times 10^3 \quad (23)$$

In contrast to the other tissues, blubber mass residuals increased positively with body condition (Fig. 6B). Blubber mass ($M_{\mathrm{Blubber},i}$) could be estimated from the body length (BL_i, Fig. 7A) and body condition (BC_i, Fig. 7C) of a whale (i):

$$M_{\mathrm{Blubber},i} = \{(1+BC_i)\times\exp[-4.115+3.016\times\log(BL_i)] - \frac{M_{\mathrm{Muscle},i}}{D_{\mathrm{Muscle}}} - \frac{M_{\mathrm{Viscera},i}}{D_{\mathrm{Viscera}}} - \frac{M_{\mathrm{Bones},i}}{D_{\mathrm{Bones}}}\} \times D_{\mathrm{Blubber}} \quad (24)$$

or if written out in full:

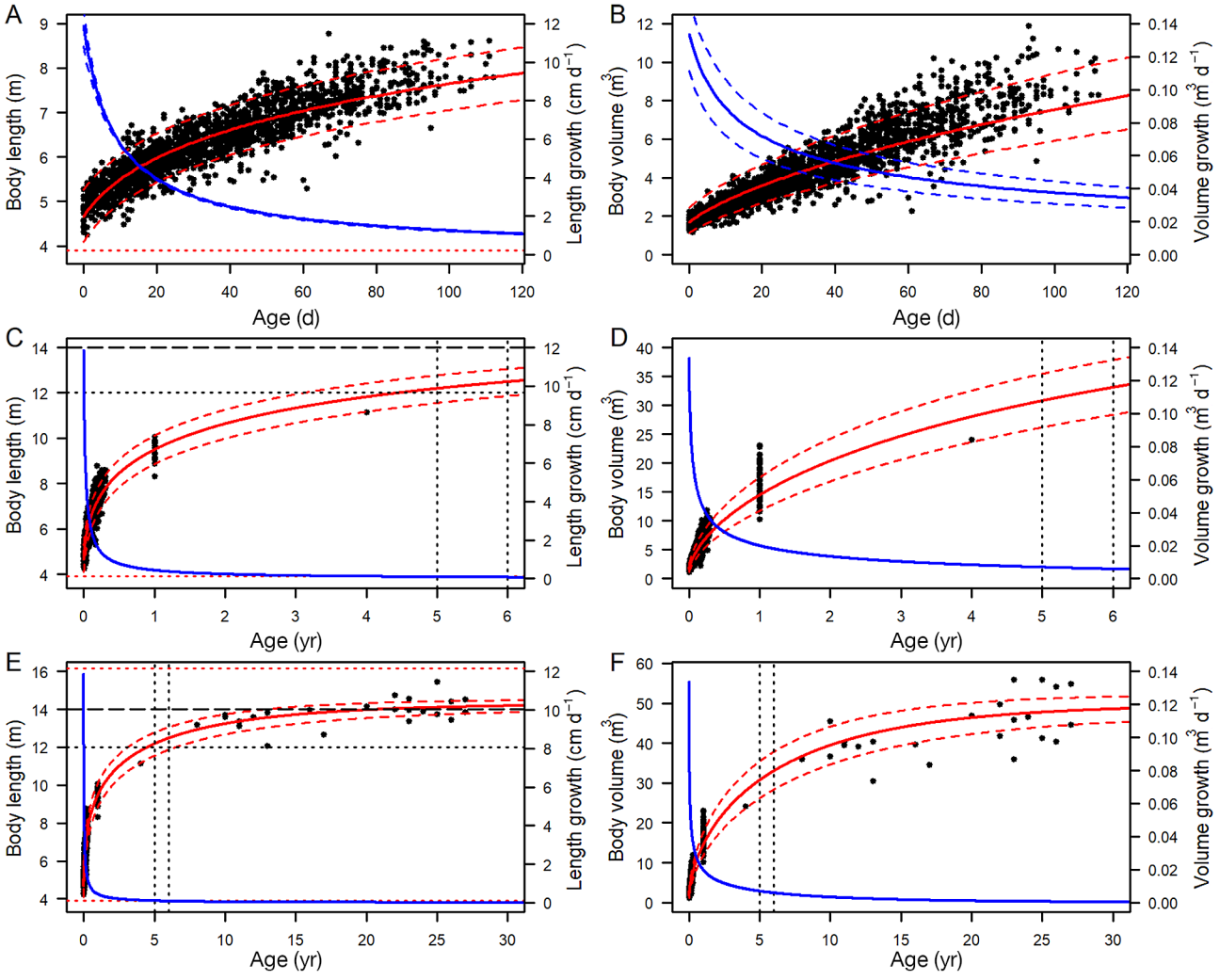

Fig. 5. Length-at-age (left column) and volume-at-age (right column) growth curves for southern right whales in South Australia across (A,B) the first 4 mo (120 d) after birth, (C,D) from birth to sexual maturation and (E,F) the full age range of the raw data. The red solid lines show the predicted body lengths (left column) and body volumes (right column) from a Richards growth curve (non-transformed). The blue solid lines show the corresponding growth rates for body length and body volume, respectively, across the same age range. The dashed lines represent the 95% confidence intervals resulting from the bootstrap resampling. The dotted red horizontal lines show the minimum (3.9 m) and maximum (16.2 m) body lengths measured in this study. The dashed black horizontal line shows the mean length (14.0 m) of mature whales. The dotted black horizontal line shows the minimum length at sexual maturity (12.0 m) and the 2 dotted black vertical lines show the age at sexual maturity (5 yr) and minimum age at first parturition (6 yr) for the South Australian population. n = 2035 measurements from 205 individuals

$$M_{\text{Blubber},i} = \left\{(1+BC_i)\times\exp[-4.115+3.016\times\log(BL_i)] - \frac{\exp[-4.115+3.016\times\log(BL_i)]\times 0.282\times 10^3}{960} - \frac{\exp[-4.115+3.016\times\log(BL_i)]\times 0.102\times 10^3}{930} - \frac{\exp[-4.115+3.016\times\log(BL_i)]\times 0.125\times 10^3}{720}\right\}\times 700 \quad (25)$$

For an animal in average body condition ($BC = 0$), the relative mass of each tissue was 36.8% blubber, 35.0% muscle, 12.7% visceral tissue and 15.5% bones (Fig. 7D). The relative mass of each tissue varied considerably with the body condition of the whales, with the relative mass of blubber increasing with body condition, while the other tissues decreased (Fig. 7D). Consequently, the average tissue density ($D_{total,i}$) of SRWs decreased non-linearly with body condition, from 850 kg m^{-3} at a body condition of −30% (lowest measured BC) to 766 kg m^{-3} at a body condition of 60% (highest measured BC) (Fig. 7B). The tissue density for an animal of average body condition ($BC = 0$) was 805 kg m^{-3} (Fig. 7B).

By combining the volume-at-age curve (Eq. 20) with the tissue mass-at-length relationships (Eqs. 21–24), tissue specific mass-at-age curves could be obtained (Fig. 8A):

$$M_{\text{Muscle},t} = \exp\{-4.115 + 3.016 \times \log[14.286(1-e^{-0.106(t-(-0.018))})^{0.179}]\} \times 0.282 \times 10^3 \quad (26)$$

$$M_{\text{Viscera},t} = \exp\{-4.115 + 3.016 \times \log[14.286(1-e^{-0.106(t-(-0.018))})^{0.179}]\} \times 0.102 \times 10^3 \quad (27)$$

$$M_{\text{Bones},t} = \exp\{-4.115 + 3.016 \times \log[14.286(1-e^{-0.106(t-(-0.018))})^{0.179}]\} \times 0.125 \times 10^3 \quad (28)$$

$$M_{\text{Blubber},t} = \{(1+BC_i)\times \exp\{-4.115+3.016\times\log[14.286\ (1-e^{-0.106(t-(-0.018))})^{0.179}]\} - \frac{M_{\text{Muscle},i}}{960} - \frac{M_{\text{Viscera},i}}{930} - \frac{M_{\text{Bones},i}}{720}\} \times 700 \quad (29)$$

which together equal the total mass-at-age of SRWs (Fig. 8A, Table 4; Table S1):

$$M_t = M_{\text{Muscle},t} + M_{\text{Viscera},t} + M_{\text{Bones},t} + M_{\text{Blubber},t} \quad (30)$$

This mass-at-age curve represents the growth in structural body mass of SRWs and does not account for seasonal variations in body condition. The rate of growth in body mass (in kg d^{-1}) of SRWs decreased from 108.0 (95% CI: 90.6–123.7) at birth, to 50.0 (40.7–59.7) at 1 mo of age, 27.8 (23.0–32.7) at 4 mo (start of southern migration), 16.1 (13.7–18.4) at 1 yr (weaning), 5.5 (5.2–5.8) at the age of sexual maturity (5 yr), 2.6 (2.5–2.7) at 10 yr, to 0.3 (0.2–0.4) at 30 yr (Fig. 8, Table 4; Table S1). For tissue-specific growth rates, see Table S2.

3.7. Energetic cost of growth

Assuming a mean blubber lipid and protein concentration of 62.6 and 10.2%, respectively, the energy required for blubber growth was 27 163 kJ kg^{-1} (Table 1). Muscle had an assumed mean lipid and protein concentration of 11.4 and 22.1%, respectively, and the energy required for muscle growth was 9732 kJ kg^{-1} (Table 1). Visceral tissue was modelled to have a mean lipid and protein concentration of 75.8 and 3.7%, respectively, and the energy required for visceral tissue growth was 30 845 kJ kg^{-1} (Table 1). Finally, using a mean bone lipid and protein concentration of 21.8 and 24.8%, respectively, the energy required for bone growth was 14 482 kJ kg^{-1} (Table 1). In combination with the relative mass of each tissue type (36.8% blubber, 35.0% muscle,

Table 3. Summary of predicted body lengths of southern right whales from different growth models and age-variable transformations (square-root, log and cube-root). Values presented in the same row as the model name represent predictions from the non-transformed model. Missing values indicate that the model did not converge

Growth model	Length at birth (age = 0 yr)	Length at minimum age of sexual maturity (age = 5 yr)	Length at minimum age of first parturition (age = 6 yr)	Asymptotic length (age = 30 yr)
von Bertalanffy	5.43	12.15	12.15	12.15
Square-root	4.35	12.43	12.70	13.99
Log	–	–	–	–
Cube-root	3.55	11.82	12.14	14.83
Richards	4.71	12.32	12.61	14.08
Square-root	4.30	12.36	12.63	14.08
Log	–	–	–	–
Cube-root	3.78	12.14	12.44	14.39
Logistic	5.23	10.56	10.56	10.56
Square-root	4.74	12.88	13.05	13.45
Log	0.00	11.51	11.81	14.77
Cube-root	3.97	12.42	12.69	14.07
Gompertz	5.25	10.86	10.86	10.86
Square-root	4.57	12.71	12.93	13.67
Log	0.00	13.69	13.69	13.69
Cube-root	3.78	12.15	12.44	14.39
Modified Gompertz	5.25	10.86	10.86	10.86
Square-root	4.57	12.71	12.93	13.67
Log	0.00	11.50	11.79	14.70
Cube-root	3.78	12.15	12.44	14.39

Table 4. Predicted mean body length, volume, mass and energy content of southern right whales at different ages (D: days, Y: years), and associated daily growth rates in length, volume, mass and energy (cost of growth). Estimates are based on an animal in average body condition (*BC* = 0), and hence represents the structural growth (not including energy deposition) of whales. For error estimates, see Table S1. For tissue-specific growth rates, see Table S2. Ages denoted with an asterisk are extrapolations beyond the age range of the data set (assuming a longevity of ~80 yr)

Age	Length (m)	Length growth (cm d^{-1})	Volume (m^3)	Volume growth (l d^{-1})	Mass (kg)	Mass growth (kg d^{-1})	Energy content (GJ)	Cost of growth (MJ d^{-1})
D-0	4.66	11.95	1.69	134.15	1360	108.00	27	2111.9
D-1	4.78	10.71	1.82	126.18	1468	101.59	29	1986.5
D-2	4.88	9.73	1.95	119.54	1570	96.24	31	1881.9
D-3	4.98	8.93	2.07	113.89	1666	91.69	33	1793.0
D-4	5.07	8.26	2.18	109.01	1758	87.76	34	1716.1
D-5	5.15	7.69	2.29	104.73	1845	84.31	36	1648.7
D-10	5.49	5.78	2.78	89.18	2239	71.80	44	1404.0
D-15	5.76	4.68	3.21	79.15	2581	63.72	50	1246.0
D-20	5.98	3.95	3.59	71.97	2887	57.94	56	1133.0
D-25	6.16	3.43	3.93	66.49	3168	53.53	62	1046.8
D-30	6.33	3.05	4.26	62.13	3428	50.02	67	978.2
D-60	7.04	1.86	5.87	46.98	4726	37.82	92	739.6
D-90	7.52	1.37	7.16	39.37	5764	31.69	113	619.7
D-120	7.88	1.09	8.27	34.55	6654	27.81	130	543.8
D-150	8.18	0.91	9.25	31.13	7447	25.06	146	490.0
D-180	8.44	0.79	10.14	28.53	8167	22.97	160	449.1
D-210	8.66	0.69	10.97	26.46	8831	21.30	173	416.6
D-240	8.85	0.62	11.74	24.76	9450	19.94	185	389.9
D-270	9.03	0.56	12.46	23.33	10030	18.79	196	367.4
D-300	9.19	0.51	13.14	22.11	10579	17.80	207	348.0
D-330	9.34	0.47	13.79	21.04	11101	16.94	217	331.2
Y-1	9.50	0.43	14.51	19.94	11678	16.06	228	314.0
Y-2	10.64	0.23	20.41	13.41	16433	10.80	321	211.1
Y-3	11.33	0.16	24.68	10.26	19870	8.26	389	161.5
Y-4	11.82	0.12	28.04	8.28	22576	6.66	441	130.3
Y-5	12.19	0.09	30.79	6.87	24792	5.53	485	108.2
Y-6	12.49	0.07	33.10	5.81	26650	4.68	521	91.5
Y-7	12.73	0.06	35.07	4.98	28232	4.01	552	78.4
Y-8	12.93	0.05	36.76	4.30	29592	3.46	579	67.7
Y-9	13.10	0.04	38.22	3.74	30772	3.01	602	58.9
Y-10	13.24	0.04	39.50	3.27	31801	2.63	622	51.5
Y-11	13.36	0.03	40.62	2.87	32702	2.31	639	45.3
Y-12	13.47	0.03	41.61	2.53	33496	2.04	655	39.9
Y-13	13.56	0.02	42.48	2.24	34196	1.80	669	35.2
Y-14	13.64	0.02	43.24	1.98	34815	1.60	681	31.2
Y-15	13.72	0.02	43.93	1.76	35364	1.42	692	27.7
Y-20	13.96	0.01	46.36	0.99	37325	0.80	730	15.6
Y-30	14.18	0.00	48.55	0.33	39083	0.27	764	5.2
Y-40*	14.25	0.00	49.28	0.11	39676	0.09	776	1.8
Y-50*	14.27	0.00	49.54	0.04	39880	0.03	780	0.6
Y-60*	14.28	0.00	49.62	0.01	39950	0.01	781	0.2
Y-70*	14.28	0.00	49.65	0.00	39975	0.00	782	0.1
Y-80*	14.29	0.00	49.66	0.00	39983	0.00	782	0.0

12.7% viscera and 15.5% bones), the estimated cost of growth was 19564 kJ kg^{-1} body mass.

The daily energy requirement (in MJ d^{-1}) for growth for SRWs was 2112 (95%CI: 1771–2420) at birth, 978 (796–1167) at 1 mo of age, 544 (450–640) at 4 mo, 314 (267–360) at 1 yr, 108 (101–113) at the age of sexual maturity, 51.5 (48.7–52.8) at 10 yr and 5.2 (3.3–7.8) at 30 yr (Fig. 8, Table 4; Table S1). For tissue-specific masses and growth rates, see Table S2. For energetic content and cost of growth of different tissues, see Table S3. The assumed lipid and protein concentration in the different tissues (blubber, muscle, viscera and bones) had a large effect on the estimated cumulative growth cost of SRWs through their lives (Fig. S1), with estimates ranging from 458 to 995 GJ, which equals a doubling in energetic costs for growth.

Based on the average lipid and protein concentrations of each tissue (Table 1), the cost of growing to 30 yr of age was 764.3 GJ (711.8–813.2 GJ) (Table 4).

4. DISCUSSION

This study presents estimates of the energetic costs of somatic growth in SRWs, based on recent (2016–2019) morphometric data from a seemingly healthy (i.e. growing) population (Charlton 2017, Charlton et al. 2018, Smith et al. 2021). Our bioenergetic estimates comprise the lipid and protein concentrations of blubber, muscle, viscera and bone tissue (although bone protein concentration was based on a single fin whale sample), standardized against an average body condition (BC = 0). The cost estimates hence represent the total (all tissues) energetic costs of somatic growth, which does not account for seasonal (tissue deposition and catabolism) or ontogenetic variation (e.g. early offspring fattening) in body condition, which are both pronounced in SRWs (Christiansen et al. 2018). This separation between structural and reserve mass will facilitate the use of dynamic energy budget models to study right whale bioenergetics and predict population consequences of disturbance (e.g. climate change) (Pirotta et al. 2018, 2019).

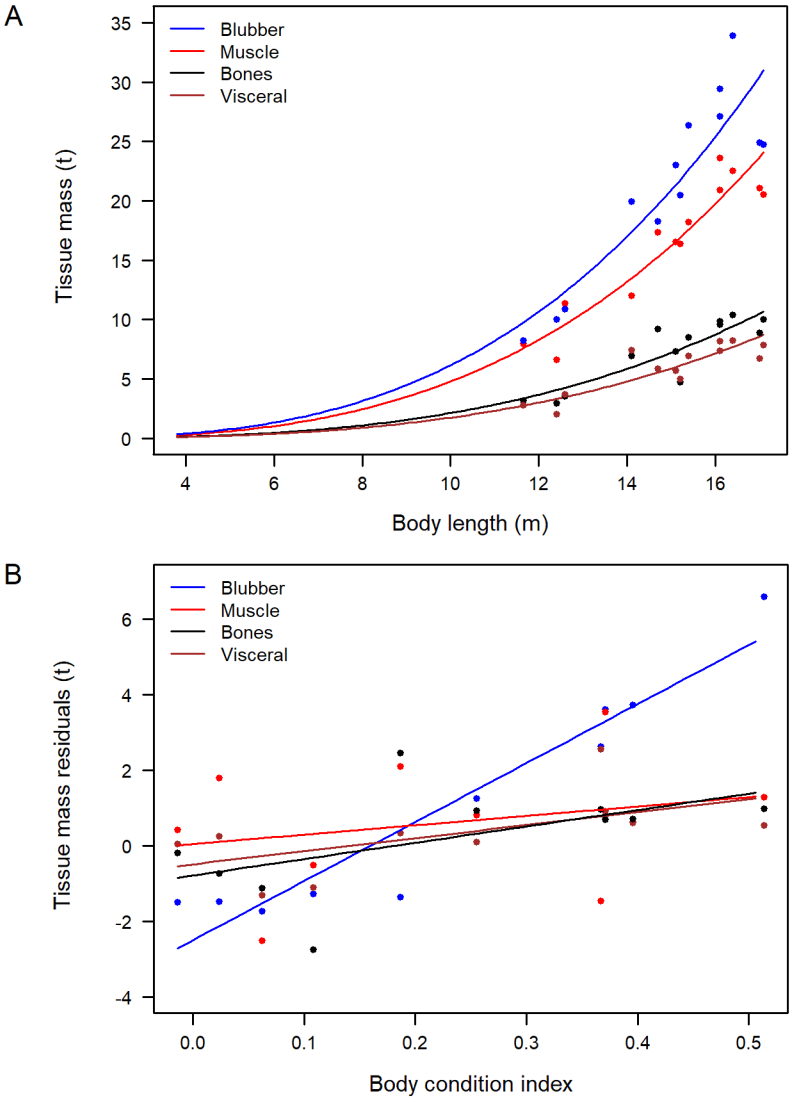

Fig. 6. (A) North Pacific right whale tissue mass as a function of body length. The solid lines correspond to the predicted tissue mass of each tissue type (see key) based on fixed tissue composition (36.3% blubber, 28.2% muscle, 10.2% viscera and 12.5% bone). (B) Tissue mass residual values as a function of body condition. The solid lines represent the fitted values of tissue-specific linear models. Only blubber residuals were significantly affected by body condition; n = 13 whales. Data obtained from Omura et al. (1969)

4.1. Somatic growth patterns

As is characteristic for baleen whales, somatic growth of SRWs was most rapid early in life, with calves doubling their relative body length from birth to weaning (1 yr), from 4.7 to 9.5 m (Table 4) or from 33 to 66% of their asymptotic length (14.3 m). Our growth model realistically captured the birth lengths of SRWs, with predicted lengths ranging from 4.1 to 5.3 m (95% CI), which is similar to the predicted birth lengths based on maternal length (Eq. 6; Christiansen et al. 2022), which across the length range of lactating females (11.7–16.2 m) results in birth lengths from 4.2 to 5.5 m. Calf growth rates from birth to 4 mo of age (the upper age range of calves when they depart the calving grounds) were also similar between the Richards growth model (1.2–6.6 cm d^{-1}, when averaging estimates over 20 d) and the estimated individual calf growth rates (1.7–5.6 cm d^{-1}), and also similar to estimates reported for SRWs from Argentina (3.5 cm d^{-1}; Whitehead & Payne 1981) and South Africa (2.8 cm d^{-1}; Best & Rüther 1992). Yearlings ranged in body length from 8.9 to 9.9 m in South Africa (Best & Rüther 1992), which was similar to the model predictions of 8.9 to 10.1 m for South Australia. SRWs in South Aus-

tralia reach sexual maturity at a minimum age of 5 yr (Charlton 2017), when they are predicted to be between 11.6 and 12.8 m in length. The mean predicted length at earliest age of sexual maturity (12.2 m, or 85% asymptotic length) corresponds well with the expected length of sexual maturity in cetaceans, which is believed to be ~85% of their asymptotic length (Laws 1956). The predicted minimum lengths of SRWs at minimum age of first parturition (6 yr; Charlton 2017) was between 11.9 and 13.1 m, which corresponds well with the minimum observed length of 11.7 m for lactating females. After reaching the minimum length of sexual maturity, the growth rate of SRWs slowed down markedly, with animals reaching 95% of their asymptotic length already at 13 yr of age. Marine mammals have indeterminate growth (Deutsch et al. 1994, Trites & Bigg 1996), which means that including a model parameter for asymptotic length is conceptually wrong. In our model, however, the asymptotic length was not reached until 70 or 80 yr of modelled age, which in practice resulted in an indeterminate growth model. Cube-root transforming the age variable in the growth models also resulted in indeterminate growth patterns for most models (Figs. S5–S9).

The allometric growth of different body parts (head size, distance to blowhole and fluke width) for SRWs were closely related to the length at weaning (~8.8 m) and minimum length at sexual maturity (~12.0 m). The strongest relationship was found between head length and body length, which differed significantly between calves, juveniles and adults, and could be used to classify whales into these 3 reproductive classes by using thresh-

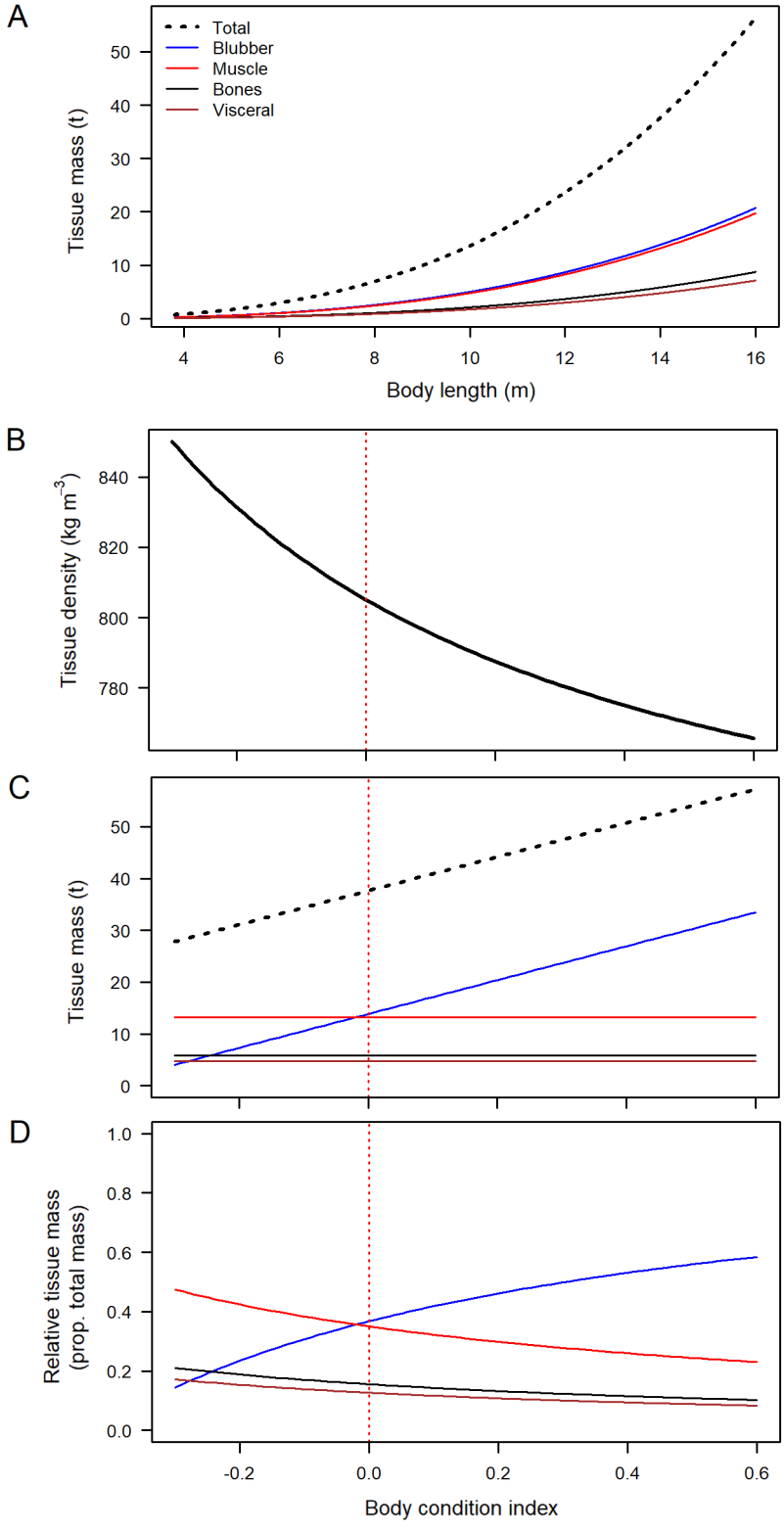

Fig. 7. (A) Southern right whale predicted tissue mass as a function of body length. The blubber mass represents an animal in average body condition ($BC = 0$). (B) Average tissue density as a function of body condition. (C) Tissue mass as a function of body condition for an average sized (14 m long) southern right whale. (D) Relative tissue mass (proportion of total mass) as a function of body condition. In A, C and D, the type of tissue is indicated by the line colour (see key). In B, C and D, the dotted vertical red line indicates an animal of average body condition ($BC = 0$)

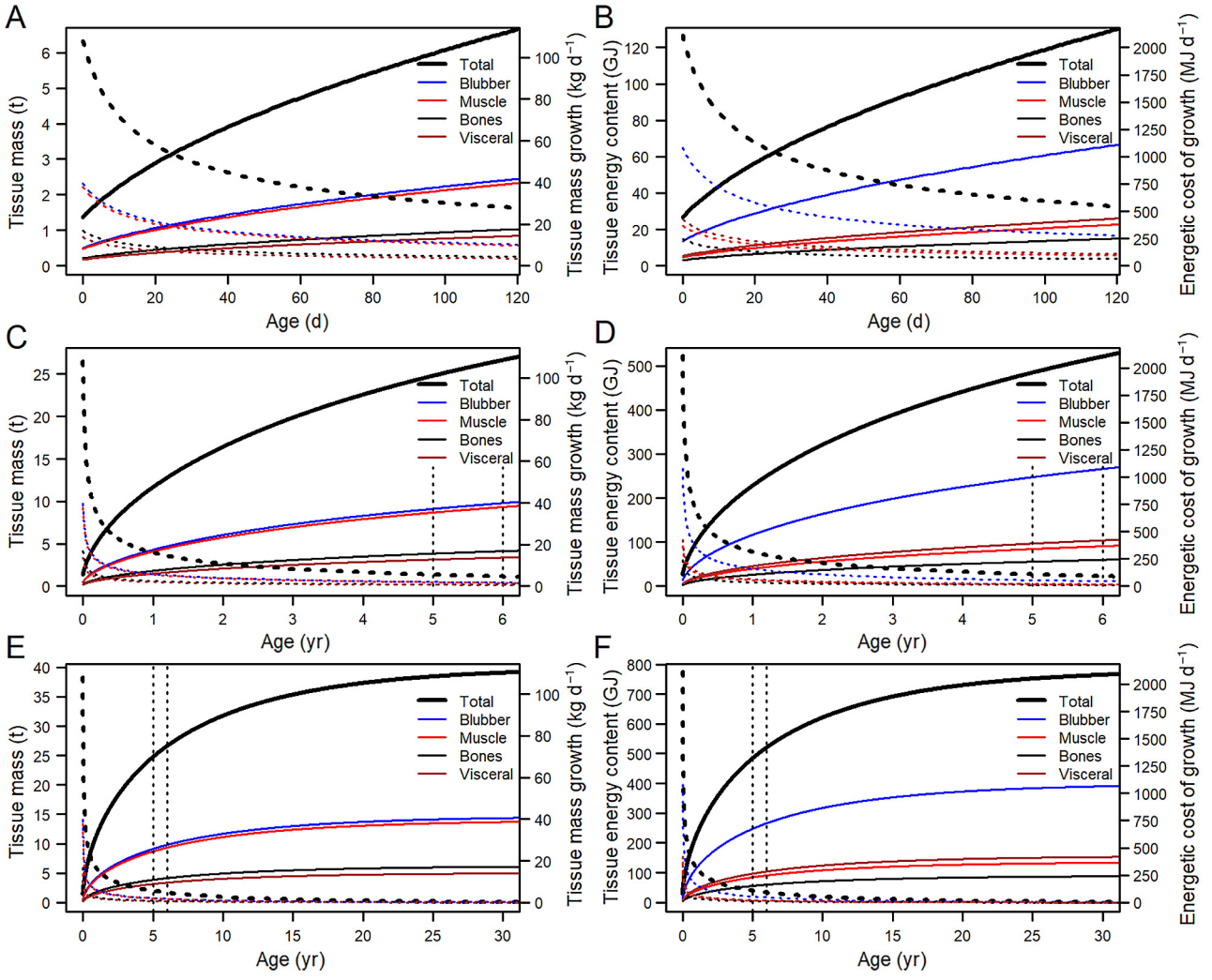

Fig. 8. Mass-at-age (left column) and energy-content-at-age (right column) curves for southern right whales (A,B) across the first 4 mos (120 d) after birth, (C,D) from birth to sexual maturation and (E,F) across the full age range of the raw data. The solid lines show the predicted masses (left column) and energy contents (right column) of the different tissue types (see key). The dotted lines show the corresponding mass growth rates (left column) and energetic costs of growth (right column) for the different tissue types (see key) across the same age range. The 2 dotted black vertical lines show the age at sexual maturity (5 yr) and minimum age at first parturition (6 yr) for the South Australian population

old values of 20.4 and 22.9%BL. Such classification thresholds have great value, since they do not require data on the absolute size (length) of the animals, and can hence be used for aerial photographs taken at unknown altitude (e.g. opportunistic data).

The somatic growth of NARWs was described using a 2-phased Gompertz model (Fortune et al. 2021). The model of Fortune et al. (2021) needed to be split into 2 phases, the first describing early growth from 0 to 1.65 yr and the second describing growth from 1.65 to 30.5 yr. In our study, we were able to fit a single model to describe the entire growth pattern of SRWs, from birth to 27 yr of age. While our growth model produced realistic estimates of SRW length-at-age, we were unable to incorporate sex as a covariate in our model to account for the sexual dimorphism that exists in baleen whales (Mesnick & Ralls 2018). Fortune et al. (2021) found that sexual dimorphism appears to occur near sexual maturity in NARWs, with adult females being 4% larger on average than adult males. Although the Western sub-population of SRWs in Australia is recovering at or near the maximum biological rate (Smith et al. 2021), the mean apparent calving interval in South Australia has increased from 3 to 4 yr from the period of 1996–2014 to 2015–2020 (Charlton et al. 2021), which could indicate some density-dependent effect being at play. Still, given that most

of the rapid growth in SRWs occurs before 6 yr of age, our length-at-age data should be representative of a recovering population that is not impeded by food constraints (is far from its carrying capacity), and hence be close to the upper growth rate limit for SRWs. Even during favourable conditions, however, individual variation in growth rates is apparent. Christiansen et al. (2018) showed that the growth rate of SRW calves varies considerably, as a function of the amount of energy invested by their mothers, which in turn is determined by the absolute size (length) and body condition of the mothers. Yearlings also varied a lot in body length, which could reflect differences in energy investment by their mothers during the preceding feeding season and/or the ability of calves to complementary feed during the preweaning period. To account for this individual variation in somatic growth, one approach would be to artificially adjust the parameter values of the Richards growth model until they cover the upper range of values in observed body length of SRWs, and use that as the upper physiological (genetic) threshold for growth. The lower limits for somatic growth in SRWs is likely to be much lower than that observed in this study, since somatic growth can be significantly stunted due to malnutrition, as evident from the decline in body lengths of NARWs over the past 4 decades (Stewart et al. 2021). In regards to body volume, our growth model only describes structural growth (BC = 0), which means that the large observed deviations from the predicted growth curve is due to individual variation in body condition (Fig. 5). This is particularly noticeable for yearlings, which are significantly fatter than other reproductive classes (Christiansen et al. 2020b).

4.2. Body tissue composition and energy content

The body tissue composition of right whales (based on data from NPRWs) was 36.8% blubber, 35.0% muscle, 12.7% viscera and 15.5% bones, relative to their structural mass (BC = 0). The estimated bone mass of SRWs was similar to that of other baleen whales, and did not vary with the length or body condition of the whales (Nishiwaki 1950, Lockyer et al. 1985, Lockyer & Waters 1986, Vikingsson et al. 2013b). While studies of fin and sei whales have shown some variation in lipid and protein concentration of bone tissue, no corresponding variation in bone mass has been found, possibly as a consequence of lipid oil displacing water in bone tissue (Lockyer & Waters 1986, Lockyer 1987). Visceral mass was also constant relative to structural mass, and did not vary with body condition in right whales. While other baleen whales show relatively small seasonal variation in visceral mass, its energetic content varies significantly over the year, and visceral tissue consequently plays an important role as an energy reserve, especially for pregnant females, in these species (Lockyer et al. 1984, Vikingsson 1995, Vikingsson et al. 2013b, Gunnlaugsson 2020). Similar to visceral tissue, the proportion of muscle tissue in right whales did not vary with the body condition of the animal. This is in strong contrast to other baleen whale species, including minke, sei, fin and blue whales, which all show large seasonal variations in both the mass and relative energy content of muscle (Lockyer et al. 1985, Lockyer 1987, Vikingsson 1995, Niæss et al. 1998, Vikingsson et al. 2013a,b, Gunnlaugsson 2020). Instead, blubber was the only tissue that varied seasonally with body condition, which indicates that blubber is the most important tissue for seasonal energy storage in right whales. This is consistent with the findings by Lockyer (1976), who showed that right whales have a significantly higher proportion of blubber compared to other species of baleen whales. With the proportion of blubber volume varying with body condition, the average body tissue density of right whales varied from 850 kg m^{-3} at a body condition of −30% (our lowest estimate) to 766 kg m^{-3} at a body condition of 60% (our highest estimate). This seasonal variation in body density should significantly influence the buoyancy of the whales (Aoki et al. 2021), which in turn could influence swimming kinematics, cost of transport and foraging energetics (on the feeding grounds) (Aoki et al. 2011, P. Miller et al. 2012). The tissue density for an animal of average body condition (BC = 0) was 805 kg m^{-3}. This is higher than the estimate of 754.63 kg m^{-3} reported by Christiansen et al. (2019), and is likely due to the latter study not taking into account variations in tissue composition with variations in individual body condition. Instead, Christiansen et al. (2019) used the mean body density of the NPRWs sampled by Omura et al. (1969), which were all in very good body condition.

Unfortunately, we did not have empirical data on the energy content of different body tissues of SRWs, and instead we based our growth cost estimates on values published for fin, sei and minke whales (Lockyer et al. 1985, Lockyer 1987, Vikingsson 1990, Vikingsson et al. 2013a). Those studies reported large variations in lipid concentration for blubber, muscle and visceral tissues, as well as protein concentration in blubber. Only a single value for bone

protein concentration was available, and hence we could not account for variation in the energy content of this tissue due to protein. While we found strong negative correlations between lipid and protein concentrations in the blubber, muscle and visceral tissues in fin, sei and minke whales, we were unable to determine potential relationships in energy content across tissues, or probable relationships between morphological body condition (e.g. body girth) and tissue energy content. As a result, the confidence interval around our estimate of energetic cost of growth in SRWs from birth to 30 yr of age varied from 458 to 995 GJ. Using the extreme values of this estimate will have significant implications when modelling the bioenergetics of right whales, and hence we encourage researchers to collect empirical data on lipid and protein concentrations of right whale tissues from stranding records and incidental catches of the species along with body length, girth and blubber thickness. While blubber biopsy sampling can be used to measure the lipid and protein concentration in the outer blubber layer of free-living whales (the blubber layer of most juvenile/adult baleen whales is too thick to obtain a full depth biopsy), studies have shown that outer blubber lipid concentrations do not relate to the morphological body condition of baleen whales (Kershaw et al. 2019, Christiansen et al. 2020b), and we hence discourage extrapolation of such data to the entire body of whales.

4.3. Methodological implications

Animal growth curves are important not only to determine the cost of growth throughout the lifetime of an individual, but also a necessary step to estimate other components of its energetic budget, including field metabolic rates (costs for body maintenance) and relative costs of reproduction, which both vary with body mass (Kleiber 1947, Christiansen et al. 2018). We used a non-lethal approach to obtain size-at-age curves for SRWs, by combining aerial photogrammetry methods with long-term sighting histories, similar to Fortune et al. (2021) and Stewart et al. (2021). Aerial photogrammetry data can be obtained using either UAVs (Durban et al. 2015, Christiansen et al. 2016) or conventional aircraft (Best & Rüther 1992, Perryman & Lynn 2002, C. Miller et al. 2012), and allows for repeated measurements of the same animals over time to investigate somatic growth both at an individual and population level (Christiansen et al. 2018, Stewart et al. 2021). In our study, the age of individual whales was obtained from the GABRWS long-term monitoring programme, which has been collecting identification data annually since 1991. For populations lacking long-term sighting data, DNA methylation-based biomarkers could potentially be used to age individuals (Polanowski et al. 2014, Bors et al. 2021). However, to accurately capture the rapid early growth rate of baleen whales, as demonstrated in this study, the accuracy of such estimates needs to be improved significantly. Notwithstanding, we encourage similar non-lethal approaches to be applied to other baleen whale species and populations, ideally as part of ongoing monitoring programmes, to provide updated estimates of growth rates and costs over time (Stewart et al. 2021). Such data are becoming increasingly important, as forecasted rapid changes in the marine environment, due to natural and anthropogenic factors (including climate change) (Crain et al. 2008, Hoegh-Guldberg & Bruno 2010, Doney et al. 2012, Hawkins et al. 2017), are likely to lead to reductions in prey availability and body size of whales, and can subsequently impact species recovery (Isaac 2009, Gardner et al. 2011).

4.4. Management implications

The HoB SRWs are part of the 'western' Australian subpopulation, which currently numbers around 2500–3000 individuals (Smith et al. 2021). Since systematic aerial surveys began in 1993, the subpopulation has been growing rapidly at around 4.5–5.2% yr^{-1} (Smith et al. 2021). Anthropogenic disturbance to this subpopulation is believed to be low compared to other SRW populations (DSEWPaC 2012, Azizeh et al. 2021). Based on this, the growth curve presented in this paper is representative of a healthy (growing) population, which is unlikely to be limited by low prey availability or impeded by human disturbance. In contrast, the NARW population is experiencing high anthropogenic pressure from shipping and fisheries (Knowlton et al. 2012, Kraus et al. 2016), and has been declining since 2011 (Pace et al. 2017). A recent study found that the somatic growth rates of NARWs have declined over the past 4 decades (Stewart et al. 2021), likely as a result of malnutrition resulting from a reduction in prey availability (Meyer-Gutbrod et al. 2021) and an increase in anthropogenic stressors (Knowlton et al. 2012, Kraus et al. 2016). The difference in the somatic growth between our study population and that of the NARW demonstrates the likely energetic effect that anthropogenic disturbance can have on baleen whales, and

the importance of better understanding the bioenergetics of large whales to be able to predict the population consequences of future disturbances, including climate change.

Author contributions. F.C. conceived and designed the study. F.C. and L.B. secured funding for the UAV work and S.B. and C.C. obtained funding for the long-term monitoring project. F.C. coordinated and carried out the UAV fieldwork. Long-term sighting history data was provided by C.C. and S.B. Data processing, analyses and interpretation was carried out by F.C. F.C. wrote the manuscript with input from all authors.

Acknowledgements. This study was funded by the US Office of Naval Research Marine Mammals Program (award nos. N00014-17-1-3018 and N00014-21-1-2601) and the World Wide Fund for Nature Australia, Murdoch University and Aarhus Institute of Advanced Studies. F.C. received funding from the AIAS-COFUND II fellowship programme that is supported by the Marie Skłodowska-Curie actions under the European Union's Horizon 2020 (grant agreement no. 754513) and the Aarhus University Research Foundation. This paper represents HIMB and SOEST contribution nos. 1882 and 11488, respectively. The Great Australian Bight Right Whale Study Research funding was provided by Murphy Australia Oil Pty. Ltd., Santos Ltd. and Karoon Gas for 2016–2019 and in-kind support provided by Curtin University Centre for Marine Science and Technology. We are also grateful for the private contribution by C. Farrell (www.chrisfarrellnaturephotography.com.au). We thank the Aboriginal Lands Trust, Yalata Land Management and Far West Coast Aboriginal Corporation for allowing us access to Aboriginal lands to carry out this research. All research was carried out under research permits from the Department for Environment and Water (DEW), South Australia (M26501-2, M26501-4, M26501-5 and M26501-6); Marine Parks permits (MR00082-3-V, MO00082-4-R, MO00082-5-R and MO00082-6-R); and animal ethics permits from DEW (4/2016) and Murdoch University (O2819/16). The UAV was operated under UAV operator's certificates with the necessary remotely piloted aircraft system licences in accordance with regulations by the Australian Civil Aviation Safety Authority. We thank Interspacial Aviation Services Pty. Ltd. (www.interspacialaviation.com.au) for training in UAV operations and safety. We thank A. Morrison and all of the research assistants and volunteers for help with data collection and processing. Finally, we thank handling Editor Dr. R. Suryan and reviewers C.H. Lockyer and K.C. Bierlich for their constructive comments which helped to improve this manuscript.

LITERATURE CITED

Aguilar A, Borrell A (1990) Patterns of lipid content and stratification in the blubber of fin whales (*Balaenoptera physalus*). J Mammal 71:544–554

Aoki K, Watanabe YY, Crocker DE, Robinson PW and others (2011) Northern elephant seals adjust gliding and stroking patterns with changes in buoyancy: validation of at-sea metrics of body density. J Exp Biol 214: 2973–2987

Aoki K, Isojunno S, Bellot C, Iwata T and others (2021) Aerial photogrammetry and tag-derived tissue density reveal patterns of lipid-store body condition of humpback whales on their feeding grounds. Proc R Soc B 288: 20202307

Azizeh TR, Sprogis KR, Soley R, Nielsen MLK and others (2021) Acute and chronic behavioral effects of kelp gull micropredation on southern right whale mother–calf pairs off Península Valdés, Argentina. Mar Ecol Prog Ser 668:133–148

Baty F, Ritz C, Charles S, Brutsche M, Flandrois JP, Delignette-Muller ML (2015) A toolbox for nonlinear regression in R: the package nlstools. J Stat Softw 66:1–21

Best PB, Rüther H (1992) Aerial photogrammetry of southern right whales, *Eubalaena australis*. J Zool (Lond) 228: 595–614

Blueweiss L, Fox H, Kudzma V, Nakashima D, Peters R, Sams S (1978) Relationships between body size and some life history parameters. Oecologia 37:257–272

Bors EK, Baker CS, Wade PR, O'Neill KB and others (2021) An epigenetic clock to estimate the age of living beluga whales. Evol Appl 14:1263–1273

Brodie PF (1975) Cetacean energetics, an overview of intraspecific size variation. Ecology 56:152–161

Brody S (1968) Bioenergetics and growth. Hafner, New York, NY

Charlton CM (2017) Population demographics of southern right whales (*Eubalaena australis*) in Southern Australia. PhD thesis, Curtin University, Bentley

Charlton C, Bannister J, McCauley RD, Brownell RL Jr, Ward R, Salgado-Kent C, Burnell S (2018) Demographic parameters of southern right whales (*Eubalaena australis*) off Australia. Document SC/67B/INFO/22. International Whaling Commission, Cambridge

Charlton C, Marsh O, Shannessy BO, McCauley R, Burnell S (2021) Long term southern right whale research at Head of Bight, South Australia 1991–2020 — Annual Field Report 2020. Document SC/68C/SH11_Rev01. International Whaling Commission, Cambridge

Charrondiere UR, Haytowitz DB, Stadlmayr B (2012) FAO/INFOODS density database, version 2.0. www.fao.org/3/ap815e/ap815e.pdf

Chittleborough RG (1955) Puberty, physical maturity, and relative growth of the female humpback whale, *Megaptera nodosa* (Bonnaterre), on the Western Australian coast. Aust J Mar Freshw Res 6:315–327

Christiansen F, Dujon AM, Sprogis KR, Arnould JPY, Bejder L (2016) Noninvasive unmanned aerial vehicle provides estimates of the energetic cost of reproduction in humpback whales. Ecosphere 7:e01468

Christiansen F, Vivier F, Charlton C, Ward R, Amerson A, Burnell S, Bejder L (2018) Maternal body size and condition determine calf growth rates in southern right whales. Mar Ecol Prog Ser 592:267–281

Christiansen F, Sironi M, Moore MJ, Di Martino M and others (2019) Estimating body mass of free-living whales using aerial photogrammetry and 3D volumetrics. Methods Ecol Evol 10:2034–2044

Christiansen F, Dawson SM, Durban JW, Fearnbach H and others (2020a) Population comparison of right whale body condition reveals poor state of the North Atlantic right whale. Mar Ecol Prog Ser 640:1–16

Christiansen F, Sprogis KR, Gross J, Castrillon J, Warick HA, Leunissen E, Bengtson Nash S (2020b) Variation in outer blubber lipid concentration does not reflect morphological body condition in humpback whales. J Exp Biol 223: jeb213769

Christiansen F, Uhart MM, Bejder L, Clapham P and others (2022) Foetal growth, birth size and energetic cost of gestation in southern right whales. J Physiol, doi:10.1113/jp282351

Cooke JG, Clapham PJ (2018) North Pacific right whale. *Eubalaena japonica*. IUCN Red List of Threatened Species: e.T41711A50380694

Crain CM, Kroeker K, Halpern BS (2008) Interactive and cumulative effects of multiple human stressors in marine systems. Ecol Lett 11:1304–1315

Deutsch CJ, Crocker DE, Costa DP (1994) Sex- and age-related variation in reproductive effort of Northern elephant seals. In: Le Boeuf BJ, Laws RM (eds) Elephant seals: population ecology, behavior, and physiology. University of California Press, Berkeley, CA, p 169–210

Dmitriew CM (2011) The evolution of growth trajectories: What limits growth rate? Biol Rev Camb Philos Soc 86: 97–116

Doney SC, Ruckelshaus M, Duffy JE, Barry JP and others (2012) Climate change impacts on marine ecosystems. Annu Rev Mar Sci 4:11–37

Douhard F, Gaillard JM, Pellerin M, Jacob L, Lemaître JF (2017) The cost of growing large: costs of post-weaning growth on body mass senescence in a wild mammal. Oikos 126:1329–1338

DSEWPaC (Department of Sustainability, Environment, Water, Population and Communities) (2012) Conservation management plan for the Southern right whale: a recovery plan under the Environmental protection and biodiversity conservation act 1999, 2011–2021. DSWEPaC, Canberra

Durban JW, Fearnbach H, Barrett-Lennard LG, Perryman WL, Leroi DJ (2015) Photogrammetry of killer whales using a small hexacopter launched at sea. J Unmanned Veh Syst 3:131–135

Elzhov TV, Mullen KM, Spiess AN, Bolker B (2016) Minpack.lm: R interface to the Levenberg-Marquardt nonlinear least-squares algorithm found in MINPACK, plus support for bounds. R Package version 1.2-1. https://cran.r-project.org/web/packages/minpack.lm/index.html

Fortune SME, Moore MJ, Perryman WL, Trites AW (2021) Body growth of North Atlantic right whales (*Eubalaena glacialis*) revisited. Mar Mammal Sci 37:433–447

Frazer JFD, Huggett ASG (1973) Specific foetal growth rates of cetaceans. J Zool 169:111–126

Gardner JL, Peters A, Kearney MR, Joseph L, Heinsohn R (2011) Declining body size: a third universal response to warming? Trends Ecol Evol 26:285–291

Gompertz B (1825) On the nature of the function expressive of the law of human mortality, and on the new mode of determining the value of life contingencies. Philos Trans R Soc Lond 115:513–583

Gunnlaugsson T (2020) Spatial and temporal variation in body mass and the blubber, muscle and visceral fat content of North Atlantic common minke whales. J Cetacean Res Manag 21:59–70

Hamilton PK, Knowlton AR, Marx MK, Kraus SD (1998) Age structure and longevity in North Atlantic right whales *Eubalaena glacialis* and their relation to reproduction. Mar Ecol Prog Ser 171:285–292

Harding KC, Salmon M, Teilmann J, Dietz R, Harkonen T (2018) Population wide decline in somatic growth in harbor seals — early signs of density dependence. Front Ecol Evol 6:59

Hawkins ER, Harcourt R, Bejder L, Brooks LO and others (2017) Best practice framework and principles for monitoring the effect of coastal development on marine mammals. Front Mar Sci 4:59

Hoegh-Guldberg O, Bruno JF (2010) The impact of climate change on the world's marine ecosystems. Science 328: 1523–1528

Isaac JL (2009) Effects of climate change on life history: implications for extinction risk in mammals. Endang Species Res 7:115–123

Kaufmann KW (1981) Fitting and using growth curves. Oecologia 49:293–299

Kershaw JL, Brownlow A, Ramp CA, Miller PJO, Hall AJ (2019) Assessing cetacean body condition: Is total lipid content in blubber biopsies a useful monitoring tool? Aquat Conserv 29:271–282

Kjellqwist SA, Haug T, Øritsland T (1995) Trends in age-composition, growth and reproductive parameters of Barents Sea harp seals, *Phoca groenlandica*. ICES J Mar Sci 52:197–208

Kleiber M (1947) Body size and metabolic rate. Physiol Rev 27:511–541

Knowlton AR, Hamilton PK, Marx MK, Pettis HM, Kraus SD (2012) Monitoring North Atlantic right whale *Eubalaena glacialis* entanglement rates: a 30 yr retrospective. Mar Ecol Prog Ser 466:293–302

Kraus SD, Kenney RD, Mayo CA, McLellan WA, Moore MJ, Nowacek DP (2016) Recent scientific publications cast doubt on North Atlantic right whale future. Front Mar Sci 3:137

Laird AK (1966) Postnatal growth of birds and mammals. Growth 30:349–363

Laws RM (1956) Growth and sexual maturity in aquatic mammals. Nature 178:193–194

Lepage D, Gauthier G, Reed A (1998) Seasonal variation in growth of greater snow goose goslings: the role of food supply. Oecologia 114:226–235

Lockyer C (1976) Body weights of some species of large whales. ICES J Mar Sci 36:259–273

Lockyer C (1981a) Estimation of the energy costs of growth, maintenance and reproduction in the female minke whale, (*Balaenoptera acutorostrata*), from the Southern hemisphere. Document SC/32/Mi19. The Scientific Committee of the International Whaling Commission, Cambridge

Lockyer C (1981b) Growth and energy budgets of large baleen whales from the southern hemisphere. In: Clark JG (ed) Mammals in the seas. FAO Fish Ser 5, Vol 3. General papers and large cetaceans. FAO, Rome, p 379–487

Lockyer C (1984) Review of baleen whale (Mysticeti) reproduction and implications for management. Rep Int Whaling Comm Spec Issue 6:27–50

Lockyer C (1987) Evaluation of the role of fat reserves in relation to the ecology of North Atlantic fin and sei whales. In: Huntley AC, Costa DP, Worthy GAJ, Castellini MA (eds) Approaches to marine mammal energetics. Spec Publ 1. Society for Marine Mammalogy, Lawrence, KS, p 183–203

Lockyer C, Waters TD (1986) Weights and anatomical measurements of north eastern Atlantic fin (*Balaenoptera physalus*, Linnaeus) and sei (*B. borealis*, Lesson) whales. Mar Mamm Sci 2:169–185

Lockyer CH, McConnell LC, Waters TD (1984) The biochemical composition of fin whale blubber. Can J Zool 62:2553–2562

Lockyer C, McConnell LC, Waters TD (1985) Body condition in terms of anatomical and biochemical assessment of body fat in North Atlantic fin and sei whales. Can J Zool 63:2328–2338

Madsen T, Shine R (2000) Silver spoons and snake body sizes: prey availability early in life influences long-term growth rates of freeranging pythons. J Anim Ecol 69: 952–958

Mesnick S, Ralls K (2018) Sexual dimorphism. In: Würsig B, Thewissen JGM, Kovacs KM (eds) Encyclopedia of marine mammals, 3rd edn. Academic Press, San Diego, CA, p 848–853

Meyer-Gutbrod EL, Greene CH, Davies KTA, Johns DG (2021) Ocean regime shift is driving collapse of the North Atlantic right whale population. Oceanography 34:22–31

Millar JS (1977) Adaptive features of mammalian reproduction. Evolution 31:370–386

Miller CA, Best PB, Perryman WL, Baumgartner MF, Moore MJ (2012) Body shape changes associated with reproductive status, nutritive condition and growth in right whales *Eubalaena glacialis* and *E. australis.* Mar Ecol Prog Ser 459:135–156

Miller PJO, Biuw M, Watanabe YY, Thompson D, Fedak MA (2012) Sink fast and swim harder! Round trip cost-of-transport for buoyant divers. J Exp Biol 215:3622–3630

Mori M, Butterworth DS (2006) A first step towards modelling the krill–predator dynamics of the Antarctic ecosystem. CCAMLR Sci 13:217–277

Niæss A, Haug T, Nilssen EM (1998) Seasonal variation in body condition and muscular lipid contents in Northeast Atlantic minke whale *Balaenoptera acutorostrata.* Sarsia 83:211–218

Nishiwaki M (1950) On the body weight of whales. Sci Rep Whales Res Inst 4:184–209

Omura H, Ohsumi S, Nemoto T, Nasu K, Kasuya T (1969) Black right whales in the North Pacific. Sci Rep Whales Res Inst 21:1–78

Pace RM, Corkeron PJ, Kraus SD (2017) State-space mark–recapture estimates reveal a recent decline in abundance of North Atlantic right whales. Ecol Evol 7:8730–8741

Pauly D (1979) Gill size and temperature as governing factors in fish growth: a generalization of von Bertalanffy's growth formula. Berichte aus dem Institut für Meereskunde an der Christian-Albrechts-Universität, No. 63. Institut für Meereskunde, Kiel

Payne R, Brazier O, Dorsey EM, Perkins JS, Rowntree VJ, Titus A (1983) External features in southern right whales (*Eubalaena australis*) and their use in identifying individuals. In: Payne R (ed) Communication and behavior of whales. Westview Press, Boulder, CO, p 371–445

Perryman WL, Lynn MS (2002) Evaluation of nutritive condition and reproductive status of migrating gray whales (*Eschrichtius robustus*) based on analysis of photogrammetric data. J Cetacean Res Manag 4:155–164

Peters RH (1983) The ecological implications of body size. Cambridge University Press, Cambridge

Pirotta E, Mangel M, Costa DP, Mate B and others (2018) A dynamic state model of migratory behavior and physiology to assess the consequences of environmental variation and anthropogenic disturbance on marine vertebrates. Am Nat 191:E40–E56

Pirotta E, Mangel M, Costa DP, Goldbogen J and others (2019) Anthropogenic disturbance in a changing environment: modelling lifetime reproductive success to predict the consequences of multiple stressors on a migratory population. Oikos 128:1340–1357

Polanowski AM, Robbins J, Chandler D, Jarman SN (2014) Epigenetic estimation of age in humpback whales. Mol Ecol Resour 14:976–987

Promislow DEL (1993) On size and survival: progress and pitfalls in the allometry of life span. J Gerontol 48: B115–B123

R Core Team (2020) R: a language and environment for statistical computing. R Foundation for Statistical Computing, Vienna

Reiss MJ (1991) The allometry of growth and reproduction. Cambridge University Press, Cambridge

Ricker WE (1979) Growth rates and models. In: Hoar WS, Randall DJ, Bret JR (eds) Fish physiology: bioenergetics and growth, Vol 8. Academic Press, Orlando, FL, p 677–743

Schmidt-Nielsen K (1984) Scaling: Why is animal size so important? Cambridge University Press, Cambridge

Smith JN, Jones D, Travouillon K, Kelly N, Double M, Bannister JL (2021) Monitoring population dynamics of 'western' right whales off southern Australia 2018–2021 — final report on activities for 2020. Report to the National Environmental Science Program, Marine Biodiversity Hub, Western Australian Museum, Perth

Stewart JD, Durban JW, Knowlton AR, Lynn MS and others (2021) Decreasing body lengths in North Atlantic right whales. Curr Biol 31:3174–3179.E3

Trites AW, Bigg MA (1996) Physical growth of northern fur seals (*Callorhinus ursinus*): seasonal fluctuations and migratory influences. J Zool (Lond) 238:459–482

Tulloch VJD, Plagányi ÉE, Brown C, Richardson AJ, Matear R (2019) Future recovery of baleen whales is imperiled by climate change. Glob Change Biol 25:1263–1281

Vikingsson GA (1990) Energetic studies on fin and sei whales caught off Iceland. Rep Int Whaling Comm 40: 365–373

Vikingsson GA (1995) Body condition of fin whales during summer off Iceland. In: Blix AS, Walløe L, Ulltang Ø (eds) Whales, seals, fish and man. Elsevier Science, Amsterdam, p 361–369

Vikingsson GA, Auðunsson GA, Elvarsson BÞ, Gunnlaugsson T (2013a) Energy storage in common minke whales (*Balaenoptera acutorostrata*) in Icelandic waters 2003–2007. Chemical composition of tissues and organs. Document SC/F13/SP10. Reports of the International Whaling Commission. IWC, Reykjavik

Vikingsson GA, Auðunsson GA, Gunnlaugsson T, Elvarsson BÞ, Haug T, Christiansen F, Lydersen C (2013b) Energy deposition of common minke whales (*Balaenoptera acutorostrata*) during the feeding season in Icelandic waters. Document SC/65a/O02. Reports of the International Whaling Commission. IWC, Cambridge

von Bertalanffy L (1938) A quantitative theory of organic growth (inquiries on growth laws. II). Hum Biol 10: 181–213

Whitehead H, Payne R (1981) New techniques for assessing populations of right whales without killing them. In: Clark JG (ed) Mammals in the seas. FAO Fish Ser 5, Vol 3. General papers and large cetaceans. FAO, Rome, p 189–209

Wootton JT (1987) The effects of body mass, phylogeny, habitat, and trophic level on mammalian age at first reproduction. Evolution 41:732–749

Editorial responsibility: Robert M. Suryan, Juneau, Alaska, USA
Reviewed by: K. Bierlich, C. H. Lockyer

Submitted: September 29, 2021
Accepted: January 31, 2022
Proofs received from author(s): April 4, 2022